energy&fuels

pubs.acs.org/EF Review

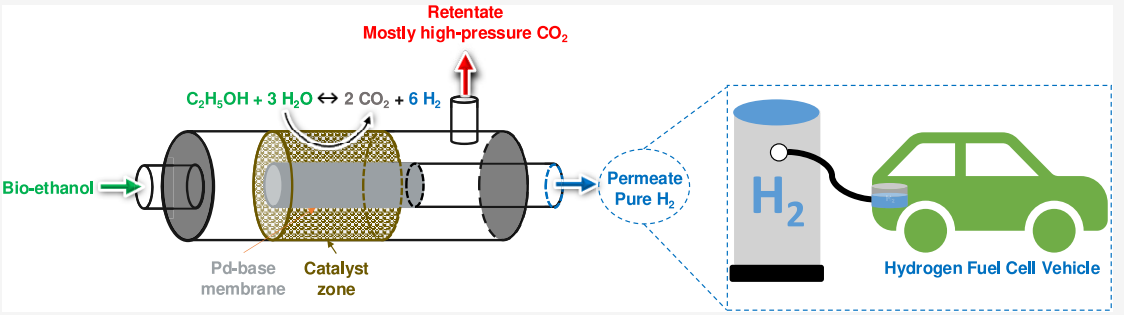
Low-Carbon Hydrogen Production via Ethanol Reforming Reactions in Membrane Reactors: Recent Advances and Future Directions

Published as part of Energy & Fuels special issue "Celebrating Women in Energy Research".

Omid Jazani, Moses Adejumo, Mohamed A. Elharati, and Simona Liguori*

Cite This: *Energy Fuels* 2024, 38, 19992–20014 Read Online

ACCESS | Metrics & More | Article Recommendations



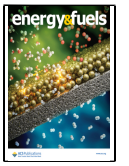
ABSTRACT: The emission of greenhouse gases (GHGs) has escalated to unprecedented levels due to the extensive use of fossil fuels for industrial development and population growth. Consequently, the transition to clean and renewable energy sources is critical for mitigating climate change. Hydrogen is considered a promising energy carrier that can be produced from both conventional (fossil fuels) and renewable resources (biofuels and water). Among renewable sources, ethanol is favored over other bioalcohols because it has a high energy content and is less toxic than hydrocarbon fuels. In addition, ethanol reforming represents a viable method of efficiently producing renewable hydrogen. To enhance this process, innovative technologies have been developed, particularly through the use of a membrane reactor (MR) technology. In MRs, the reaction and separation processes occur simultaneously, which improves the selectivity and yield while reducing operating conditions and preventing coke formation. This study aims to highlight recent advancements in ethanol reforming reactions—including steam reforming, partial oxidation, and autothermal reforming reactions—to produce renewable, low-carbon hydrogen using MR technology. In particular, the central focus is to provide a comprehensive analysis of the performance of different MRs, shedding light on their efficacy, scalability, and potential limitations in the context of renewable hydrogen production from ethanol reforming. By exploring these aspects, this study attempts to inform strategic decisions and advancements in sustainable energy technologies, facilitating the transition toward a greener, more resilient energy landscape.

Downloaded via QUAID-I-AZAM UNIV ISLAMABAD on July 23, 2026 at 15:26:54 (UTC).
See https://pubs.acs.org/sharingguidelines for options on how to legitimately share published articles.

1. INTRODUCTION

The continuous growth of the global economy and population has escalated the demand for energy production.[1,2] Fossil fuels, including oil, gas, and coal, account for approximately 80% of global energy production.[3,4] Consequently, the combustion of these fuels significantly contributes to the emission of greenhouse gases (GHGs) into the atmosphere. According to a report by the International Energy Agency (IEA), CO_2 emissions from the energy sector reached 36.8 gigatonnes in 2022.[5,6] Figure 1(a) and 1(b) illustrates the global distribution of CO_2 emissions and energy consumption across various sectors in the same year. Notably, the power or electricity generation sector is the largest emitter, contributing 42% (15.5 gigatonnes) of the total due to its heavy reliance on fossil fuels and the continued operation of numerous coal-fired power plants worldwide. The transportation sector ranks as the third largest emitter of CO_2, although it is the largest consumer of energy. This is attributed to developments in fuel efficiency and engine technology and the expansion of electric public transportation in major cities. The release of CO_2 is a significant driver of global temperature increases, leading to climate change.[7,8] The Intergovernmental Panel on Climate Change (IPCC) has recommended limiting the rise in global temperatures to below 1.5 °C relative to preindustrial levels

Received: June 7, 2024
Revised: October 1, 2024
Accepted: October 3, 2024
Published: October 22, 2024



© 2024 American Chemical Society

https://doi.org/10.1021/acs.energyfuels.4c02755
Energy Fuels 2024, 38, 19992–20014

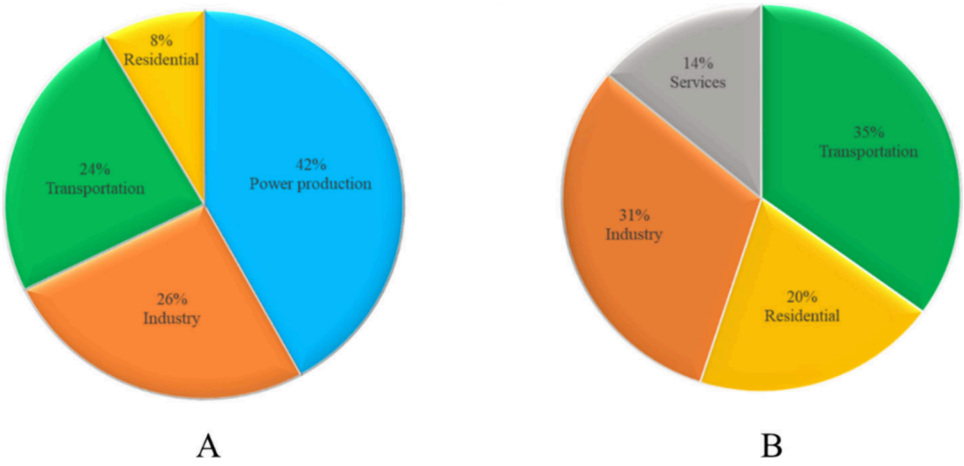


Figure 1. (a) Global CO_2 emission by sectors. (b) Global energy consumption by sectors[5,6]

and achieving net-zero carbon emissions by 2050 to mitigate the impacts of global warming and climate change.[7,8]

Today, there is an urgent need to shift energy production from fossil fuels to clean, sustainable, and renewable sources, which include solar, wind, geothermal, and hydropower.[3,9] However, these sources generate intermittent energy, relying on weather conditions and geographic location, and their long-term energy storage poses significant challenges.[2,3] As an alternative, hydrogen is seen as a promising carbon-free energy vector due to its high energy conversion efficiency, high storage capacity, abundant and renewable production sources, regenerability, and zero emissions during its use. Although the hydrogen atom is the most abundant element on the earth, it is rare to find it in molecular form, so it has to be produced form sources containing hydrogen (e.g., hydrocarbon and water components).[7,10−12] Currently, 96% of hydrogen is produced by fossil fuel processes, and about 4% is generated by renewable processes.[13,14] Figure 2 shows the production

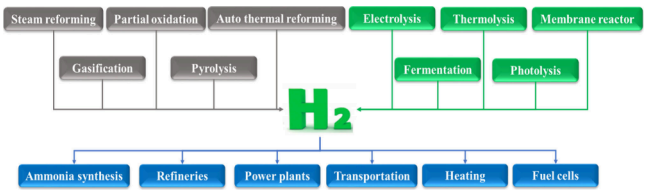


Figure 2. Hydrogen production methods and their application.

processes for generating hydrogen along with its applications. Among these, the steam methane reforming (SMR) process generates 50% of hydrogen globally produced. This commercial process has higher efficiency, lower cost, and lower operating conditions than other processes.[9,15,16] However, it is very energy-intensive and emits 9−12 kg of CO_2 per kg of H_2 produced. To reduce CO_2 emissions, carbon capture utilization and sequestration (CCUS) units can be deployed[17] or alternative ways, including the use of bioalcohols and biofeedstock can be used.[18] Alcohols like methanol and ethanol, for instance, can be used for steam-reforming reactions instead of methane.[19] Among the bioalcohols, ethanol has shown great potential due to its high hydrogen content, high reactivity with water at higher temperatures, sustainable fuel, easy transportation, and free from poisonous content for catalysts.[20−22] It can be produced in large quantities from fermentation of sugar containing materials, which is usually avoided to not compete with food, or biowaste materials; thus, the cost of generation is lower than methanol. Also, ethanol has a higher reactivity than methanol, and it could produce more hydrogen by reacting with both atomic oxygen and hydroxyl radicals. The use of ethanol in fuel cells offers the significant advantage of being nearly CO_2 neutral.[23] This is because the CO_2 generated during steam reforming process is offset by its consumption during biomass growth, thereby creating a nearly closed carbon cycle (zero emission).[21,24,25] The ethanol steam reforming (ESR) process has been extensively studied by researchers using various catalysts and reactors, demonstrating advantages over other biofuels.[25−28] However, the multistep hydrogen production and separation process remains challenging due to harsh operating conditions and low efficiency.[29,30] Additionally, the ESR reaction involves several side reactions that can decrease H_2 yield and promote coke formation, making the development of new catalysts and reactors crucial to overcoming these issues.[25,27,31] Besides steam reforming, hydrogen can also be produced via partial oxidation and autothermal reforming. Moreover, generating hydrogen through biofuel reforming and capturing the resulting CO_2 can result in negative carbon emissions.[32,33]

To increase the efficiency of the process and reduce CO_2 emissions, membrane reactors (MRs) can be utilized to simultaneously produce and separate hydrogen. The use of MR technology intensifies the process, requiring less energy and, hence, reducing CO_2 emissions.[9] Indeed, MRs can operate at milder operating conditions (300−500 °C and 2−5 bar) than conventional reactors (CRs) to reach specific efficiency in terms of conversion.[9] This benefit is due to the membrane's ability to remove the desirable product from the reaction zone and shift the reaction toward further reactants consumption, a phenomenon known as the "shift effect". In addition, one of the two outlet MR streams is mainly composed of pressured CO_2, which can be further processed or captured. Another benefit is that MRs is a versatile technology, where diverse feedstocks such as methanol,[34] ethanol,[35] glycerol,[36] natural gas, acetic acid,[37] ammonia,[38] and biomethane[39] can be used to separate hydrogen. In the past few years, MRs have shown great potential for decentralized small- and medium-scale hydrogen production plants. Indeed, a few examples of MR applications in industry include Tokyo Gas company, which

https://doi.org/10.1021/acs.energyfuels.4c02755
Energy Fuels 2024, 38, 19992−20014

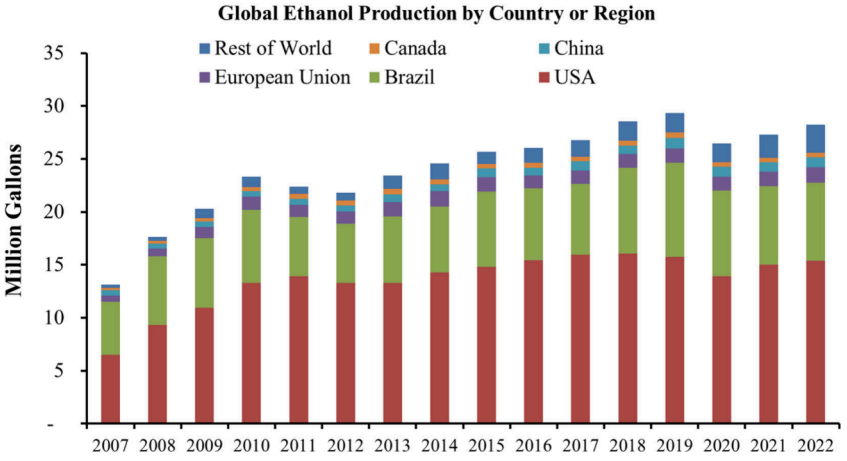


Figure 3. Ethanol production by countries from 2007 to 2022 (U.S Department of Energy − Alternative Fuel Data Center).[56]

developed the first pilot Pd MR for hydrogen production through SMR process, capable for producing 40 N m^3/h of ultrapure hydrogen,[40,41] Johnson & Matthey, Membrane Technology and Research (MTR), Kinetics Technology and more recently Tecnalia which developed a system producing 5 N m^3/h.[42]

As MRs require high-temperature operation, inorganic membranes, including metallic, ceramic, carbon, and zeolite, are considered as the optimal choice because of their high thermal and chemical stability over organic membranes.[9,43−46] Among these materials, metallic membranes have been predominantly used for hydrogen production due to their exceptional selectivity, robust mechanical and chemical stability, and compatibility with the operational temperatures required for reforming reactions. The metallic membranes for hydrogen separation include V, Nb, Ta, Pt, Pd, and metals in group III−V.[47] In particular, palladium-based MRs have been mainly studied for hydrogen production and separation under reforming reactions because of their complete selectivity toward hydrogen permeation. However, challenges such as embrittlement phenomenon, occurring by sudden changes in Pd phases (α and β) at a temperature lower than 293 °C,[42] chemical poisoning, and low thermal stability are frequently cited as the main concerns associated with the use of pure palladium (Pd) membranes.[9,43−46] To mitigate these issues, Pd is usually alloyed with other metals, such as silver (Ag), gold (Au), and copper (Cu). Adding Au and Cu, for example, enhances both physical and chemical stabilities and slightly increases hydrogen permeability. On the other hand, the addition of Ag improves hydrogen permeability and prevents the embrittlement effect at low temperatures. Consequently, Pd alloy MRs are appropriate for reforming reactions compared to pure Pd MRs.[9,43−46]

Most of the review articles in the existing literature regarding ethanol reforming reactions investigated the effect of various catalysts.[26,48−51] Only a few articles reviewed hydrogen production from ESR reaction in MRs,[52,53] and the most recent study was published in 2008 by Taghizadeh and Aghili,[52] who only analyzed the ESR in MR. As mentioned above, the ESR reaction in Pd alloy membrane reactors (MRs) presents a sustainable and clean method for hydrogen generation, utilizing renewable feedstock, operating at lower temperatures, producing ultrapure hydrogen for fuel cells, capturing CO_2, and enabling installations at needed locations, all while potentially achieving negative carbon emissions. This review aims to provide a comprehensive overview of hydrogen separation methods and recent advancements in hydrogen production through steam reforming, partial oxidation, and autothermal reactions of ethanol using various MRs. The review covers these processes under different operating conditions, reporting both experimental and modeling studies. Lastly, a brief techno-economic analysis and lyfe cycle assessment of ESR is presented, along with a discussion of the challenges and potential future research directions.

2. A BRIEF OVERVIEW OF ETHANOL PROPERTIES AND PRODUCTION METHOD

Ethanol, an organic compound with the chemical CH_3CH_2OH, is a colorless, volatile liquid with a mild odor. Its physical properties are mainly influenced by the presence of a hydroxyl group and a short carbon chain. The hydroxyl group allows ethanol to form hydrogen bonds, making it more viscous and less volatile than other compounds with a similar molecular weight.[54] Additionally, the hydroxyl group makes ethanol highly reactive, allowing it to be easily transformed into various materials through processes such as dehydrogenation, dehydration, or oxidation. Bioethanol is often produced locally where biomass is available, contributing to economic growth by providing countries with a renewable resource for fuel production. The demand for ethanol continues to rise, driven by its use as a biofuel blended with gasoline. For instance, 98% of gasoline in the U.S. contains ethanol to help oxygenate the fuel and improve its octane rating.[54]

Ethanol can be produced through both biological and chemical pathways, with the biological route being the primary method globally. Figure 3 shows ethanol production worldwide. According to the U.S. Department of Energy, ethanol production increased from 13 million gallons to 28 million gallons by 2022, with the U.S. and Brazil responsible for 80% of global production. The U.S. Department of Agriculture projects that ethanol consumption will increase by 27 million gallons by 2030 due to its use as a gasoline additive, driving further economic growth. The largest consumers of ethanol are the U.S., Brazil, and China, with consumption rates of 14.4, 7.9, and 1 million gallons, respectively.[55,56] The U.S. government supports ethanol production through incentives like direct and indirect subsidies, tax credits, and exemptions, lowering production costs and enabling producers to export ethanol for additional revenue.[57]

https://doi.org/10.1021/acs.energyfuels.4c02755
Energy Fuels 2024, 38, 19992−20014

Table 1. Advantages and Disadvantages of Conventional Hydrogen Production Processes[62−65]

Process	Advantages	Disadvantages	Efficiency	Developer
Steam reforming	Most developed technology	CO_2 emission	74−85%	Haldor Topsoe AS, Foster Wheeler Corp, and Lurgi AG
	Low operating temperature			
	Highest H_2/CO ratio			
	Highest efficiency			
	No oxygen requirement			
Thermal partial oxidation	No catalyst requirement	Complex handling process	60−75%	Texaco, Inc., and Royal Dutch/Shell
	Less desulfurization requirement	Low H_2/Co ratio		
	Low slip methane	Requiring Oxygen		
		High operating temperature		
Catalytic partial oxidation	Ideal H_2/CO ratio	Limited commercial experience	60−75%	Exxon Mobile pilot plant
	Lower processing temperature	Complex handling process		
	No need for external heat	Requiring Oxygen		
Auto thermal reforming	Required less O_2 than PO_x	Less commercial	60−75%	Lurgi, Chevron, Sasol, and Haldor Topsoe
	Low process temperature than PO_x	Required oxygen or air		

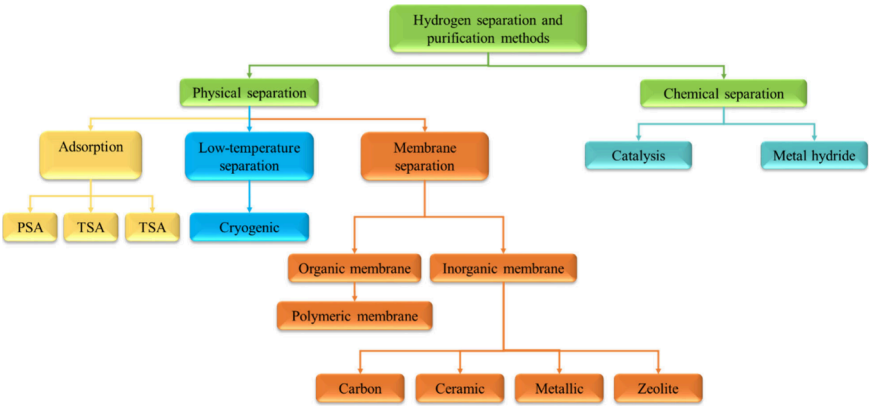


Figure 4. Hydrogen separation techniques[66]

In biological approaches, the glucose in biomass is converted to ethanol and carbon dioxide by an anaerobic process using enzymes such as cellulases and glucosidases, along with yeast, to break down the biomass into fermentable sugars. Usually, bioethanol production from agriculture and forestry waste can be categorized into three main categories: (1) sugary material like sugar cane and whey, (2) starchy material including wheat, corn, and cassava, (3) lignocellulose material like agricultural waste, and crops.[31,58]

On the chemical side, ethanol can also be produced via the catalytic conversion of synthesis gas (CO and H_2). The chemical pathways for hydrogen and ethanol production are classified into three approaches: (1) direct conversion of synthesis gas to ethanol (eqs 1), (2) conversion of synthesis to methanol followed by homologation to ethanol (eq 2), and (3) ENSOL process, the synthesis gas is converted to methanol, carbonylated to produce acetic acid, and subsequently hydrogenated to yield ethanol (eqs 3−5).[31,59,60]

$$2CO + 4H_2 \leftrightarrow C_2H_5OH + H_2O \quad \Delta H^{\circ}_{298} = 253 \text{ kJ mol}^{-1} \tag{1}$$

$$CH_3OH + CO + H_2 \leftrightarrow C_2H_5OH + H_2O \quad \Delta H^{\circ}_{298} = 165.2 \text{ kJ mol}^{-1} \tag{2}$$

$$2H_2 + CO \leftrightarrow CH_3OH \quad \Delta H^{\circ}_{298} = 90.64 \text{ kJ mol}^{-1} \tag{3}$$

$$CH_3OH + CO \leftrightarrow CH_3COOH \quad \Delta H^{\circ}_{298} = 123 \text{ kJ mol}^{-1} \tag{4}$$

$$CH_3COOH + H_2 \leftrightarrow C_2H_5OH + H_2O_2 \quad \Delta H^{\circ}_{298} = 41.7 \text{ kJ mol}^{-1} \tag{5}$$

3. CONVENTIONAL PROCESSES FOR HYDROGEN PRODUCTION AND TECHNIQUES USED FOR ITS SEPARATION

3.1. Conventional Reforming Process. In the conventional reforming processes, hydrocarbons are converted to hydrogen via catalytic reactions. The main processes are steam reforming (SR), partial oxidation (PO), and autothermal reforming reactions (ATR). If the hydrocarbons react with steam, the process is called SR and is an endothermic reaction. When they react with oxygen, it is called partial oxidation (PO) and the reaction is exothermic. The third common process, ATR, combines both SR and PO, allowing them to occur simultaneously. This integration reduces the external heat required, leading to lower energy costs and reduced CO_2 emissions associated with heat generation.[2,7,61] Table 1 compares the different reforming processes, highlighting that

https://doi.org/10.1021/acs.energyfuels.4c02755
Energy Fuels 2024, 38, 19992−20014

Table 2. Details of Each Technique Used for Hydrogen Separation[9]

Technique	Principle	Temperature (°C)	H_2 feed	Drawbacks	Benefits	H_2 recovery	H_2 purity
Cryogenic separation	Condensation of gases at low temperatures	−180	Petrochemical and refinery "off" gases	Energy-intensive Low H_2 purity	Environmentally friendly	>98%	90−98%
PSA	Selective adsorption of gases	80−180	Any H_2-rich gas	H_2 loss	High hydrogen purity	70−85%	99.99%
Solid polymer electrolyte cell	Hydrogen ions lectrolytic passage	25	H_2 produced by thermochemical cycles	Low overall cell performance	High H_2 recovery High H_2 purity	95%	99.8%
Metal hydride	Reversible reaction of hydrogen with metals to form hydrides	25	Ammonia purge gas	Relatively low hydrogen recovery	High hydrogen purity	75−95%	99.9%
Palladium membrane	Selective hydrogen diffusion	300−450	H_2 containing stream	Low mechanical resistance High cost	High purity High recovery of H_2	>99%	>99.999%
Polymer membrane	Differences in gas diffusion rate	25−100	Refineries of gases and ammonia purge gas	Low hydrogen purity	Low cost	>85%	92−98%

Reproduced with permission from ref 9. Copyright 2023 Elsevier.

SR is the most efficient, which explains its widespread use in industrial hydrogen production.

3.2. Hydrogen Separation Techniques and Membranes. The produced hydrogen exiting from the reformer needs to be purified to meet the standard requirements depending on the application. Available purification methods, which a schematic is shown in Figure 4, include adsorption processes such as pressure swing adsorption (PSA), temperature swing adsorption (TSA), cryogenic distillation, membrane separation (both organic and inorganic membrane), and metal hydrides. Choosing a suitable hydrogen separation and purification technique depends on the feed source, production method, and application. The PSA technique industrially purifies large-scale hydrogen production from SR and coal gasification. However, due to the required space and low adaptability, it is not a suitable option for small-scale hydrogen production. The cryogenic technique is an excellent alternative to remove impurities; however, it is a complex system and requires a high energy consumption. The metallic membrane and metal hydride techniques can purify hydrogen to ultragrade purity. Nevertheless, some impurities in the stream decrease the efficiency of these techniques. For decentralized small and medium applications, membranes are considered an excellent choice. Additionally, metallic membranes, such as Pd alloys membranes, can provide ultrapure hydrogen for use in proton exchange membrane fuel cells (PEMFCs).[66−68] Table 2 provides more details of each technique, showing their benefits and drawbacks. Particularly, it compares various hydrogen separation techniques based on principles, temperature ranges, feedstocks, hydrogen recovery, and purity. Membranes offer advantages for hydrogen separation compared to other techniques, as they provide high hydrogen recovery and purity while operating continuously, without requiring complex mechanical processes. Palladium-based membranes, for example, offer exceptionally high hydrogen purity (>99.999%) and recovery rates (>99%), surpassing most other methods like PSA or cryogenic separation, which either have lower purity or recovery rates. Unlike techniques such as PSA, which involves cycling pressure changes that can lead to hydrogen losses, membranes allow for a more direct, selective permeation of hydrogen, minimizing losses. Various type of membranes can be used for hydrogen separation, such as polymeric, zeolite, ceramic and metallic.[69,70]

3.2.1. Polymeric Membrane. Polymeric membranes are categorized as dense and porous and can be further divided into glassy and rubbery types. Today, they offer a competitive alternative for hydrogen separation and purification due to their high hydrogen recovery and lower operation costs. Common materials used to manufacture polymeric membranes include polysulfones (PSF), cellulose acetate, aramids, polycarbonates, poly(phenyl oxide), and polyimides. However, these conventional materials often exhibit limitations in terms of stability at high temperatures. To address these issues, advanced materials such as thermally rearranged (TR) polymers, mixed matrix membranes (MMMs), perfluoropolymers, polymerized room temperature ionic liquids (poly(RTIL)s), and polymers of intrinsic microporosity (PIMs) have been developed to enhance membrane performance. Techniques like polymer blending, copolymerization, and cross-linking are also employed to improve the quality and functionality of polymeric membranes.[71−76]

The transport mechanisms of gas through polymeric membranes vary based on the membrane morphological properties, such as pore size, and include Poiseuille (viscous) flow, Knudsen diffusion, molecular sieving, capillary condensation, and solution-diffusion for dense membranes. The driving force is usually the partial pressure gradient.[71−76] Among the different types of membranes, polymeric membranes dominate the industry due to their excellent processability, low fabrication cost, and good mechanical and chemical stability. However, polymeric membranes are not stable at temperatures higher than 110 °C, limiting their use in high-temperature processes such as reforming reactions. Additionally, they face inherent trade-off between permeability/selectivity, as well as challenges with thermal and chemical stability.[71−76]

3.2.2. Zeolite Membranes. Zeolite membranes possess properties that make them stable under harsh operating conditions, with their characteristics largely determined by the preparation methods used.[77,78] Common synthesis techniques include the embedded method, in situ hydrothermal synthesis, the seeding technique (secondary growth), the microwave method, and dry gel conversion.[76] The separation mechanism of zeolite membranes is primarily based on the molecular size and polarity. As recently reported by Amin et al.,[67] zeolite membranes are characterized by being extremely thin, pinhole-free, and reproducible, resulting in high hydrogen permeance.

https://doi.org/10.1021/acs.energyfuels.4c02755
Energy Fuels 2024, 38, 19992−20014

Table 3. Comparison of Hydrogen-Selective Membranes[9]

	Polymeric	Zeolite	Carbon	Microporous ceramic	Dense ceramic	Pd alloys
Working temperature (°C)	<100	300−500	500−900	200−600	600−900	300−600
H_2 selectivity	<10	<100	<200	<140	>1000	>1000
Poisoning issues	HCl, SOx, CO_2	Strong steam absorption	Strong adsorbing vapors, organics		H_2S	H_2S, HCl, CO
Stability issues	mechanical strength, compaction, Swelling	Acid/alkali resistance	Brittle, oxidizing	Stability in H_2O	Stability in CO_2	Metallic phase transition
Transport mechanism	Surface-diffusion; molecular sieving	Molecular sieving	Molecular sieving	Molecular sieving	Solution-diffusion	Solution-diffusion
Materials	Polymers	Silicon, aluminum	Carbon	Silica, alumina, titania, zirconia	Proton conducting ceramics	Palladium

Reproduced with permission from ref 9. Copyright 2023 Elsevier.

These membranes are capable of separating gases at temperatures ranging from 25 to 700 °C, making them highly suitable for hydrogen industrial applications. However, the relatively large pore size of zeolites compared to the kinetic diameter of hydrogen poses challenges for separating them from mixtures containing other light gas molecules.

3.2.3. Ceramic Membranes. Ceramic membranes are mainly formed from alumina, silica, zirconia, mullite, and other oxide mixtures, and they offer several advantages for gas separation, including high mechanical, thermal, and chemical stability, higher abrasion resistance, and a longer operational lifespan. However, they also have drawbacks, such as the sintering effect at higher temperatures due to their multilayer construction, higher production costs, and complex manufacturing processes. For hydrogen separation, proton conducting membranes offers 100% hydrogen selectivity, but they show reduced hydrogen permeation flux and poor chemical stability under acidic and reducing conditions.[79] Silica based one offer good hydrogen permeability, but when exposed to steam the membrane loses its separation performance.[80] Incorporating metal into proton-conducting oxides to form cermet membranes presents a promising approach for increasing hydrogen permeability.[80,81] Meng et al. reported that at 850 °C, using a 50% H_2/N_2 mixture feed and He as the sweep gas, the highest H_2 permeation flux through a cermet membrane with a 90 μm separation top layer combined with a porous substrate reached up to 0.914 mL (STP) cm^{-2} min^{-1}.[80] However, the discontinuous and uneven distribution of electronic and proton-conducting phases, along with cation interdiffusion, can result in the formation of undesirable phases during the preparation of dual-phase composite membranes.[79]

3.2.4. Metallic Membranes. Metallic membranes, generally based on palladium and its alloy, have emerged as a highly effective technology for hydrogen separation due to their unique properties of being completely selective toward this gas.[82,83] Due to Pd-cost, nonprecious metals with a body-centered cubic (BCC) structure, such as V, Cr, Nb, Ta, and Mo, have gained attention as a potential alternative to Pd for hydrogen separation. Nevertheless, these materials need a catalytic layer (usually Pd is used) on both sides to avoid oxidation and facilitate the dissociation and recombination of hydrogen atoms. They are not suitable for high operating temperatures since migration of metal elements between the core metal and the catalytic layer may prevail causing oxidation of the core metal with a corresponding decline in hydrogen permeation.[84] Nickel and iron membranes, on the other hand, are more affordable, stable, and capable of higher operating temperatures, but they present lower hydrogen permeability, necessitating thinner membranes for practical use.[82] Wang et al. fabricated nickel (Ni) hollow fiber membranes for hydrogen separation.[85] The results indicated that optimizing the microstructure H_2 flux can reach 73.17 mmol m^{-2} s^{-1} at 1000 °C. Xue et al. has demonstrated the use of Ni hollow fiber membrane for hydrogen separation in catalytic membrane reactor with stability over 84 h.[86] However, study has shown that Ni membranes can develop defects during manufacturing process when the sintering time is short and hydrogen concentration in the sintering atmosphere is low.[87] Hu et al. developed iron (Fe) hollow fiber membranes for hydrogen separation.[82] Their results showed that the membrane can achieve a H_2 flux of 23.55 mmol m^{-2} s^{-1} when operated at 850 °C with a feed containing 80% H_2. Eremeev et al. also used Ni−Cu alloy-Nd tungstate nanocomposite dense membrane deposited on asymmetric support for H_2 separation in a CMR.[88] However, the major drawback in the use of these membranes is the low hydrogen diffusion through the bulk, with limits the hydrogen permeating flux compared to the Pd membrane.[89]

As previously mentioned, Pd has gained significant attention for its unique characteristic to be completely selective toward hydrogen permeation. However, despite their high hydrogen flux and complete selectivity, Pd-pure membranes face several limitations that limit their large-scale commercialization. One major issue is their relatively low microstructural stability. Pure Pd membranes are particularly prone to poisoning by carbonaceous materials (CO and CO_2) and sulfur compounds (H_2S and SO_x), as well as embrittlement at low temperatures. The addition of metals, such as Ag, Au, Cu, and Ru to Pd has been shown to address these problems. Pd-alloy membranes exhibit improved chemical, physical, and thermal stability, higher hydrogen permeation flux, and reduced costs.[19,41,90,91]

Table 3 compares various membranes for hydrogen separation from gas mixtures. As can be seen, the working temperature and selectivity for polymeric membranes are low and unsuitable for hydrogen separation and reforming reactions. The zeolite and carbon membranes have good thermal stability for reforming reactions but low selectivity for hydrogen. Dense ceramic membrane indicates high selectivity but need high temperatures for activation and stability issues in the presence of CO_2. Thus, Pd alloy membranes are a good option to be used for hydrogen separation and reforming reactions due to complete selectivity and good stability.

https://doi.org/10.1021/acs.energyfuels.4c02755
Energy Fuels 2024, 38, 19992−20014

4. HYDROGEN SEPARATION MECHANISM BY PD-BASED MEMBRANES

Hydrogen transport in Pd-based dense membranes follows a solution-diffusion mechanism and occurs via the applied partial pressure difference between the feed and permeate sides (i.e., driving force). In the assumption of the solution-diffusion mechanism, there is no particular interaction among hydrogen molecules and membrane (i.e., differentiate from facilitated transport mechanism), and no pores exist in the membrane structure (i.e., differentiate from molecular sieving mechanism); thus, it involves six steps:[41] (1) dissociation hydrogen molecules at the interface of gas/metal, (2) hydrogen atom adsorption on the surface of the membrane, (3) hydrogen atom dissolution into a palladium matrix, (4) hydrogen atom diffusion through the membrane, (5) hydrogen atom recombination to form hydrogen molecules at the interface of metal/gas, and (6) hydrogen molecules desorption.[92] Figure 5 shows the schematic of the H_2 separation mechanism

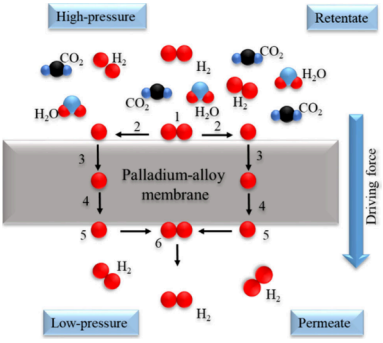


Figure 5. Schematic of the H_2 separation mechanism through a Pd-based membrane.

through a Pd-based membrane. As a result, the separation process depends on the solubility and diffusivity of hydrogen, among other gases, through the membrane. Herein, membrane permeability (P_{H2}) is the product of the solubility (S_{H2}) and diffusivity (D_{H2}) coefficients of hydrogen.

The hydrogen permeating flux through the Pd-based membrane can be expressed as[29,93,94]

$$J_{H_2} = \frac{\mathrm{Pe}_{H_2}(p^n_{H_2,\mathrm{retentate}} - p^n_{H_2,\mathrm{permeate}})}{\delta} \quad (6)$$

where J_{H_2} is the hydrogen permeating flux, Pe_{H_2} is hydrogen permeability, $p^n_{H_2,\mathrm{retentate}}$, and $p^n_{H_2,\mathrm{permeate}}$ are the hydrogen partial pressures in the retentate and permeate side, respectively, δ is the membrane thickness, and n is the dependent factor, which provides information about the rate-limiting step for hydrogen transportation by solution-diffusion mechanism, and it varies between 0.5 and 1. In the case, the n value equals 0.5, the rate-limiting step is the diffusion of the atomic hydrogen and follows Sieverts' law.[93,94] However, if the n value shifts toward 1, then the surface reaction is the rate-limiting step. In addition, the Knudsen diffusion will be involved if the selective layer is not defeat-free.[91] The hydrogen permeability depends on temperature, is independent of membrane thickness, and follows an Arrhenius-like equation[92]

$$\mathrm{Pe}_{H_2} = \mathrm{Pe}^0_{H_2}\exp\left(\frac{-E_a}{RT}\right) \quad (7)$$

where Pe^0 is the pre-exponential factor, E_a is the apparent activation energy, R is the universal gas constant, and T is the absolute temperature.[29,93,94]

The permeability term is used to evaluate the membrane performance; however, to avoid the uncertainty of the selective layer thickness measurement, the permeance (P_{H2}) term is more often used and defined as the ratio between the permeability of the hydrogen and the membrane thickness (δ)

$$P_{H_2} = \frac{\mathrm{Pe}}{\delta} \quad (8)$$

Another important parameter to evaluate the membrane performance is the ideal selectivity ($\alpha_{i/j}$), which is defined as

$$\alpha(\text{ideal selectivity}) = \frac{\text{Permeance of } H_2}{\text{Permeance of other gases}} \quad (9)$$

and other gases include Ar, He, N_2, etc.[95]

The diffusion coefficient is determined by the gas kinetic diameter, the chain spacing, and the chain segment mobility; therefore, hydrogen has a higher diffusion coefficient compared to other gases due to its small kinetic diameter, leading to faster transport through the membrane. In addition, diffusivity increases with the increment of chain segment movement and spacing. On the other hand, the solubility coefficient plays a critical role in the membrane performance (i.e., permeability and ideal selectivity) assessment, which is associated with the gas condensability (e.g., a gas with high critical temperature, the higher solubility in the membrane) and affinity to the membrane. For instance, it is easier to achieve a high ideal selectivity of H_2 due to its small kinetic diameter and high solubility in Pd selective layer.[96]

5. ETHANOL REFORMING REACTIONS

Bioethanol, or renewable ethanol, offers a promising pathway for hydrogen production due to its several benefits. It is less toxic compared to other biofeedstocks such as acetic acid and glycerol, and it can be safely transported and easily stored for on-demand production. Typically, bioethanol is classified into three categories based on its source called generations. The first generation is derived from edible crops, which is not ideal due to the food vs energy dilemma. The second generation comes from nonedible crops and waste materials, offering a more sustainable and viable option. The third generation involves innovative algae photofermentation, which holds promising potential for future bioethanol production. However, in each category, bioethanol also presents some drawbacks. For example, the presence of impurities can lead to the generation of harmful gases like CO, CO_2, and H_2S. Also, C_2 components, such as acetaldehyde, ethylene, and ethane can reduce the efficiency of catalysts and membranes. Thus, further purification is usually necessary before its use.[29,30,48,52,97]

Hydrogen can be produced from bioethanol through several reforming reactions, including SR, PO, and ATR, in both CRs and MRs. Among these methods, ESR is the most studied due to its higher hydrogen yield and process simplicity compared to both PO and ATR. Recently, considerable research efforts have focused on catalyst development for the ESR reaction, aiming to enhance conversion rates, stability, and impurity resistance while mitigating sintering and the formation of carbonaceous materials. Both noble and non-noble metals, supported by various metal oxides, have been studied to

https://doi.org/10.1021/acs.energyfuels.4c02755
Energy Fuels 2024, 38, 19992−20014

enhance catalyst performance.[24,48,25] Non-noble catalysts, such as Ni, Co, and Cu, offer low fabrication costs but are prone to poisoning by impurities and have lower activity compared with noble metals. On the other hand, noble catalysts such as Pd, Pt, Rh, Au, and Ru exhibit high activity, resistivity, and stability against impurities such as carbon and sulfuric materials, but they are expensive. Currently, bimetallic catalysts combining noble and non-noble metals have been explored to reduce manufacturing costs while improving reaction performance.[48]

In the ESR or bioethanol steam reforming (BESR) process, ethanol reacts with steam to produce hydrogen. However, various side reactions occur simultaneously, negatively affecting the performance of both the catalyst and membrane. These side reactions introduce impurities that must be carefully considered in the design and manufacturing of catalysts and reactors. The key ethanol reforming reactions, along with the anticipated undesirable side reactions, are outlined as follows:[30,52]

$$C_2H_5OH \leftrightarrow CH_4 + CO + H_2$$
$$\Delta H^\circ_{298} = 49.6 \text{ kJ mol}^{-1} \text{ (ethanol decomposition)} \quad (10)$$

$$C_2H_5OH + H_2O \leftrightarrow 2CO + 4H_2$$
$$\Delta H^\circ_{298} = 239.31 \text{ kJ mol}^{-1} \text{ (incomplete steam reforming)} \quad (11)$$

$$C_2H_5OH + 3H_2O \leftrightarrow 2CO_2 + 6H_2$$
$$\Delta H^\circ_{298} = 157 \text{ kJ mol}^{-1} \text{ (complete steam reforming)} \quad (12)$$

Side reactions:

$$C_2H_5OH \leftrightarrow CH_3CHO + H_2$$
$$\Delta H^\circ_{298} = 68.9 \text{ kJ mol}^{-1} \text{ (dehydrogenation)} \quad (13)$$

$$C_2H_5OH \leftrightarrow C_2H_4 + H_2O$$
$$\Delta H^\circ_{298} = 45.5 \text{ kJ mol}^{-1} \text{ (dehydration)} \quad (14)$$

$$2C_2H_5OH \leftrightarrow (C_2H_5)_2O + H_2O$$
$$\Delta H^\circ_{298} = -24 \text{ kJ mol}^{-1} \text{ (diethyl ether formation)} \quad (15)$$

$$CO + 3H_2 \leftrightarrow CH_4 + H_2O$$
$$\Delta H^\circ_{298} = -206.1 \text{ kJ mol}^{-1} \text{ (methanation)} \quad (16)$$

$$CO_2 + 4H_2 \leftrightarrow CH_4 + 2H_2O$$
$$\Delta H^\circ_{298} = -164.8 \text{ kJ mol}^{-1} \text{ (methanation)} \quad (17)$$

$$CH_4 + 2H_2O \leftrightarrow 4H_2 + CO_2$$
$$\Delta H^\circ_{298} = 206.1 \text{ kJ mol}^{-1} \text{ (methane steam reforming)} \quad (18)$$

$$C_2H_4O \leftrightarrow CH_4 + CO \qquad \Delta H^\circ_{298} = -164.8 \text{ kJ mol}^{-1}$$
(acetaldehyde decomposition) (19)

$$C_2H_4O + 3H_2O \leftrightarrow 2CO_2 + 5H_2$$
$$\Delta H^\circ_{298} = 186.8 \text{ kJ mol}^{-1} \text{ (acetaldehyde steam reforming)} \quad (20)$$

$$CH_3COOH + 2H_2O \leftrightarrow 2CO_2 + 4H_2$$
$$\Delta H^\circ_{298} = 131.4 \text{ kJ mol}^{-1} \text{ (acetic acid steam reforming)} \quad (21)$$

$$2C_2H_5OH \leftrightarrow CH_3COCH_3 + CO + 6H_2$$
$$\Delta H^\circ_{298} = 4.1 \text{ kJ mol}^{-1} \text{ (acetone formation)} \quad (22)$$

$$C_3H_8O_3 + 3H_2O \leftrightarrow 3CO_2 + 7H_2$$
$$\Delta H^\circ_{298} = 251 \text{ kJ mol}^{-1} \text{ (glycerol steam reforming)} \quad (23)$$

$$CO_2 + H_2 \leftrightarrow CO + H_2O$$
$$\Delta H^\circ_{298} = 41.4 \text{ kJ mol}^{-1} \text{ (reverse water gas shift reaction)} \quad (24)$$

The most significant challenge in ESR is carbon deposition, which can obstruct the catalyst active sites, reducing its activity, and hinder hydrogen dissociation on the membrane surface. This can lead to a substantial decline in the overall system performance.

$$CH_4 \leftrightarrow C + 2H_2$$
$$\Delta H^\circ_{298} = 74.9 \text{ kJ mol}^{-1} \text{ (methane decomposition)} \quad (25)$$

$$2CO \leftrightarrow CO_2 + C$$
$$\Delta H^\circ_{298} = -172.6 \text{ kJ mol}^{-1} \text{ (Boudouard reaction)} \quad (26)$$

$$C_2H_4 \leftrightarrow C + 2H_2$$
$$\Delta H^\circ_{298} = -52.3 \text{ kJ mol}^{-1} \text{ (coke formation)} \quad (27)$$

The coke formation and carbon deposition on the catalyst active surface result from methane decomposition, C_2H_4 polymerization, and Boudouard reactions. Additionally, undesirable reactions that consume generated hydrogen, such as methanation and ethanol dehydration, are problematic because their byproducts (C_2H_4 or $(C_2H_5)_2O$) contribute to the formation of carbonaceous materials. The MRs offer an effective solution for enhancing hydrogen production by minimizing undesirable side reactions occurring during ESR.[48,98] These side reactions, including methane decomposition, ethylene polymerization, and the Boudouard reaction, not only consume valuable hydrogen but also lead to catalyst deactivation. The key advantage of MRs lies in their ability to continuously separate hydrogen from the reaction system, which shifts the thermodynamic equilibrium toward greater hydrogen production while reducing the chance of side reactions. Operating at lower temperatures (350−450 °C), MRs promote the WGS reaction, converting carbon monoxide into additional hydrogen and reducing carbon deposition. Additionally, MRs suppress ethylene polymerization and improve reaction selectivity by favoring ethanol dehydrogenation, which leads to more reactive intermediates like acetaldehyde. The lower operating temperatures also prevent catalyst sintering, prolonging its lifespan and ensuring stable hydrogen output.[99]

The kinetics of ESR has been also studied using various catalysts, leading to the development of several kinetic models for the ESR process. For example, Sahoo et al.[100] investigated kinetic models on the Co catalyst with the Langmuir−Hinshelwood−Hougen−Watson mechanism, while Akande et al.[101] studied the Ni catalyst with the Eley−Rideal mechanism. Apart from non-noble catalysts, Graschinsky et al.[102] and

https://doi.org/10.1021/acs.energyfuels.4c02755
Energy Fuels 2024, 38, 19992−20014

Table 4. Kinetic models for ESR reaction using Ni-based and Co-based catalyst[105]

Rate mode	Reaction	Rate equation
1 (Ni catalyst)	Adsorption of ethanol on the surface of the catalyst	$r_a = \frac{k_0 e^{-E_a/RT}\left[C_A - \frac{C_c^2 C_D^6}{k_p C_B^3}\right]}{\left[1 + \frac{K_F C_c C_D^3}{C_B} + \frac{K_G C_c C_D^3}{C_B^2} + \frac{K_E C_c^2 C_D^6}{C_B^3}\right]}$
2 (Ni catalyst)	Dissociation of adsorbed ethanol on the catalyst to form catalysts such as CH_2O and CH_4	$r_a = \frac{k_0 e^{-E_a/RT}\left[C_A - \frac{C_c^2 C_D^6}{k_p C_B^3}\right]}{\left[1 + K_A C_A + \frac{K_F C_c C_D^3}{C_B} + \frac{K_G C_c^2 C_D^6}{C_B^3}\right]^2}$
3 (Ni catalyst)	The surface reaction of CH_2O and H_2O free vapors	$r_a = \frac{k_0 e^{-E_a/RT}\left[\frac{C_A C_B^3}{C_c C_D^4} - \frac{C_c C_D^3}{k_p}\right]}{\left[1 + K_A C_A + \frac{K_Q C_c C_B^2}{C_c C_D^3} + \frac{K_G C_c C_D^4}{C_B^2}\right]}$
4 (Ni catalyst)	The surface reaction between the CH_4 and H_2O-free vapors	$r_a = \frac{k_0 e^{-E_a/RT}\left[\frac{C_A C_B^3}{C_c C_D^4} - \frac{C_c C_D^3}{k_p}\right]}{\left[1 + K_A C_A + \frac{K_F C_c C_D^3}{C_B} + \frac{K_G C_c C_D^4}{C_c C_D^3}\right]}$
5 (Ni catalyst)	Surface rearrangement of the chemisorbed hydrogen atom	$r_a = \frac{k_0 e^{-E_a/RT}\left[\frac{C_A C_B^3}{C_D^6} - \frac{C_c^2}{k_p}\right]}{\left[1 + K_A C_A + \frac{K_F\sqrt{C_A C_B}}{C_D} + \frac{K_F\sqrt{K_G C_A}}{C_B} C_D + \frac{K_E C_A^{0.5} C_B^{1.5}}{C_D^3}\right]}$
1 (Co catalyst)	Ethanol steam reforming	$r_a = \frac{k_r K_{CH_3CH_2O}\left[\frac{p_{C_2H_5OH}}{p_{H_2}^{0.5}} - \frac{\left(\frac{1}{K_{SRE}}\right) p_{CO_2}^2 p_{H_2}^{5.5}}{p_{H2O}^3}\right][C_T]^2}{DEN^2}$
2 (Co catalyst)	Ethanol decomposition	$r_a = \frac{k_r K_{CH_3CHO}\left[\frac{p_{CO_2}^2 p_{H_2}^5}{p_{H_2O}^3} - \frac{1}{K_{ED}} p_{CH4} p_{CO}\right][C_T]^2}{DEN^2}$
3 (Co catalyst)	Water–gas shift	$r_a = \frac{k_w K_{HCOO}\left[p_{CO} p_{H_2}^{0.5} - \frac{\frac{1}{K_{WGS}} p_{H2O} p_{CO}}{p_{H_2}^{0.5}}\right][C_T]^2}{DEN^2}$

Rossetti et al.[103] studied the kinetics of ESR on Rh catalyst, and Lu et al.[104] analyzed the kinetics of Ru-based catalyst. Punase et al.[105] provided a comprehensive review of the kinetics of ESR on various catalysts. Table 4 shows several kinetic models for ESR using Ni-based and Co-based catalyst.

5.1. Ethanol Steam Reforming Reaction in MRs. MRs combine both reaction and separation simultaneously. This benefit allows us to lower operating conditions, improve conversion and yield, and lower operating cost. In addition, MRs could hinder some side reactions during ESR reactions, which improve hydrogen yield and production and reduce coke formation.[52] The following section provides a perspective on the advancements and research on hydrogen production from the ESR reaction in MRs. To compare the performance of various MRs, the following parameters are considered:

$$\text{Ethanol conversion} = \frac{\text{Ethanol}_{in} - \text{Ethanol}_{out}}{\text{Ethanol}_{out}} \times 100\% \quad (28)$$

$$\text{Hydrogen recovery} = \frac{\text{Hydrogen}_{permeate}}{\text{Hydrogen}_{permeate} + \text{Hydrogen}_{retentate}} \times 100\% \quad (29)$$

$$\text{Hydrogen yield} = \frac{\text{Hydrogen}_{produced}}{6\text{Ethanol}_{feed}} \times 100\% \quad (30)$$

$$\text{Gas hourly space velocity (GHSV)} = \frac{\text{Volumetric flow rate of feed gas}}{\text{Volume of catalyst bed}} \quad (31)$$

In the past decade, several studies have been focused on investigating the MRs performance by performing ESR using various catalysts under different operating temperatures and pressures. For instance, Hedayati et al.[106] studied ESR in a catalytic MR by using a Pd–Ag membrane and Pd–Rh/CeO_2 catalyst. Their results revealed an increase in hydrogen recovery and yield as the temperature and pressure were raised, while a decrease was observed with a higher feed molar rate and steam-to-carbon (S/C) ratio. These changes in performance are due to a combination of thermodynamics, kinetics, and membrane effects. The increase of the hydrogen recovery and yield with temperature can be attributed to three main factors: (1) ESR endothermicity—the reaction is an endothermic reaction, which is favored at higher temperatures; (2) catalyst activity—higher temperatures improve catalytic activity, resulting in increased hydrogen production; and (3) shift effect—high temperatures increase H_2 permeability across the membrane.

https://doi.org/10.1021/acs.energyfuels.4c02755
Energy Fuels 2024, 38, 19992−20014

Regarding the pressure, although the ESR results in an increased number of moles and is not favored at high pressures (thermodynamic effect), higher pressure leads to more hydrogen removal along the membrane (shift effect), as indicated by eq 1. In this case, the shift effect is more predominant than the thermodynamic effect, which improves the MR performance in terms of the hydrogen recovery and yield. Additionally, an increased feed molar ratio reduces the residence time, negatively impacting conversion and consequently decreasing both hydrogen recovery and the yield. Furthermore, increasing the S/C ratio reduces the performance, because more steam dilutes the hydrogen in the retentate side, resulting in less hydrogen permeating through the membrane.

Miyamoto et al.[107] investigated the performances of various MR types with different catalysts for ESR reactions. The Co/CeO_2 catalyst showed a better hydrogen yield at 400 °C, while the Ni/CeO_2 catalyst indicated a higher hydrogen yield at 500 °C. Because the Ni catalyst had a higher rate of methane-forming reaction than the Co catalyst at low temperatures, it led to consuming more H_2, resulting in lower hydrogen removal from the Pd−Ag membrane. The addition of Pd and Ru to the Co/CeO_2 catalyst increased both the conversion and hydrogen yield. The Pd−Co catalyst achieved higher conversion compared to the Ru−Co catalyst. However, at 350 °C, the Ru−Co catalyst attained a greater hydrogen yield than the Pd−Co catalyst due to its higher selectivity for H_2 and lower selectivity for CH_4. Moreover, different amorphous MRs with Pd alloy MRs using the Ru−Co/CeO_2 catalyst were compared for the ESR reaction at 350 °C. The results show that the order in terms of hydrogen recovery and yield is that Pd_{77}−Ag_{23} > $Ni_{40}Nb_{20}Ta_5Zr_{30}Co_5$ > $Pd_{78}Cu_6Si_{16}$. The Pd−Ag exhibits the highest performance due to higher hydrogen permeability in Pd−Ag compared to others.

Iulianelli et al.[108] investigated three different types of feed molar ratio: stoichiometric (S/C = 3), water excess (S/C = 13), and bioethanol model ($H_2O/C_2H_5OH/C_3H_8O_3/C_2H_3OOH$ = 13/1/0.04/0.18) in Pd/Al_2O_3 MR over Ni/CeO_2 catalyst. Ethanol conversion was 57% for stoichiometric, 70% for excess water, and 90% for bioethanol at 400 °C, 2 bar, and 5000 h^{-1}. The water excess and bioethanol had higher conversion because the excess steam reacted with some byproducts such as CO and CH_4. The three feeds had nearly the same purity, around 80%. However, when the pressure increased from 2 to 3 bar, the purity decreased by 10% because the Pd membrane was not completely defect-free. Hydrogen recovery was higher for the bioethanol model, reaching 62% at 400 °C and 3 bar. Further investigation of GHSV on the bioethanol conversion and H_2 recovery indicated that both decreased by 30% when GHSV was increased by 10000 h^{-1} at 400 °C and 3 bar due to a reduction in residence time. A few years later, the same authors[109] investigated Co−Pt/CeO_2−ZrO_2−Al_2O_3 bimetallic catalyst for BESR reaction in Pd/Al_2O_3 composite MR. Bioethanol conversion and H_2 recovery reached 50% and 60% at 4800 h^{-1}, 400 °C, S/C = 6/1, respectively. The effect of sulfur and phosphorus in bioethanol feed on the catalyst and membrane performance was also investigated. The MR performance was reduced. The SEM analysis showed carbon, sulfur, and phosphorus species, as well as defects on the surface of the membrane, indicating a detrimental effect of the impurities on both the catalyst and membrane.

Ma et al.[110] analyzed large-scale double-layer Pd−Au−Pd−Au membranes fabricated by sequential electroplating technique for ESR over Ni/Al_2O_3 catalyst. Ethanol conversion reached 100%, and H_2 purity was approximately 99.9% at 500 °C, S/C = 5, 5 bar, and 3.77 h^{-1}. Ruocco et al.[111] synthesized a new Pt−Ni catalyst for ESR reaction in Pd/ceramic and obtained 95% and 100% ethanol conversion at 480 and 520 °C. They obtained high conversion because the reaction was conducted at relatively high temperatures compared with the standard temperature (300−400 °C).

Santucci et al.[112] investigated three catalysts (Ru, Ni, and Pt) for ESR with a dense Pd−Ag membrane. Hydrogen yield improved with an increased pressure and feed molar ratio. For example, at 2 bar and 450 °C, it increased from 44% with S/C = 8.5 to 83% with S/C = 13. Finally, the Ru catalyst showed higher performances than Pt and Ni due to its higher activity. Mironova et al.[113] developed new catalysts, Pd−Ru, Pd−Ni, Pt−Ru, and Pt−Ni, with detonation nanodiamonds (DNDs) to investigate the ESR on dense Pd−Ru and Pd−Ru−In MRs. The Pt−Ru catalyst showed higher hydrogen recovery than Pd−Ru and Pt−Ni catalysts, reaching 36% at 500 °C in Pd−Ru MR. Moreover, in Pd−Ru−In MR, hydrogen recovery was 47% with the Pd−Ru catalyst, while the hydrogen recovery for the Pd−Ru catalyst in the Pd−Ru membrane was 22% under the same conditions due to the presence of In in the membrane. Also, Pd−Ru−In MR showed a higher performance in hydrogen yield than Pd−Ru MR at 350−500 °C and S/C = 9.[113] The same authors investigated the performance of the Pt−Ru/DND catalyst in the Pd−Rh membrane, and the hydrogen yield enhanced from 15% at 350 °C to 85% at 500 °C.

Jia et al.[114] studied the ESR reaction on Pd/ceramic composite MR packed with an Ir/CeO_2 catalyst. They showed that the presence of sweep gas enhanced the hydrogen yield and recovery due to widening hydrogen partial pressure between the retentate and permeate sides. The MR with sweep gas had a 45% higher H_2 yield than the MR without sweep gas at a pressure range of 9 to 15 bar and 500 °C. Also, H_2 recovery was 92% at 9 bar for the MR with sweep gas and 64% for the MR without sweep gas at 9 bar and 500 °C. Also, they found that the increase in sweep gas/feed flow ratio improved H_2 yield and recovery.[114] A continuous work by Jia et al.[115] compared Pd−Cu and Pd which were deposited on ceramic supports. Both MRs showed the same H_2 yield and recovery results at 400 to 600 °C and 1300 kPa. However, in terms of stability, the Pd−Cu showed better performance in terms of H_2 yield, recovery, and purity over 250 h. For instance, the purity remained stable at around 98%, while it declined from 96% to 91% in Pd MR at 600 °C and 13 bar. Moreover, it was observed that carbonaceous species inhibited H_2 permeation through the membranes. The coke formation was likely due to the higher temperature, which caused bioethanol decomposition. The H_2 permeation decreased by 40% for the Pd−Cu membrane and by 85% for the Pd membrane from their original values, indicating that the Pd−Cu membrane reactor is the superior option for the ESR reaction due to its greater resistance to carbonaceous species. Recently, Eremeev et al.[88] compared the ESR reaction in CR to Ni−Cu nanocomposite MR. They observed higher hydrogen yield in MR than CR at each operating condition investigated, except when they increased ethanol concentration. This inverse relation between H_2 recovery and ethanol concentration was due to insufficient steam. This led to coke formation from ethanol decomposition,

https://doi.org/10.1021/acs.energyfuels.4c02755
Energy Fuels 2024, 38, 19992−20014

Table 5. Summary of ESR Reaction in MRs

Membrane	Type of the MR	Support	Thickness (μm)	Catalyst	S/C	T (°C)	P (bar)	Ethanol conversion (%)	H_2 recovery (%)	Ref
$TiO_2-Al_2O_3$/Pd−Ag	Packed-bed	-	50	Ru−Al_2O_3	4.5	600	1.3	50	-	99
Ceramic/Pd−Ag	Packed-bed	-	50	Ru−Al_2O_3	4.5	600	1.3	40	-	99
Pd−Ag	Packed-bed	-	50	Ru−Al_2O_3	4.5	600	1.3	50	-	99
Pd−Ag	Packed-bed	-	50	Ru−Al_2O_3	11	400	2	88	8	116
Pd−Ag	Packed-bed	-	50	Ru−Al_2O_3	11	500	2	99	22	116
Pd−Ag	Packed-bed	-	50	Ru−Al_2O_3	3	300	1.3	18	10	117
Pd−Ag	Packed-bed	-	50	Ru−Al_2O_3	9	400	1.3	100	16	117
Pd−Ag	Packed-bed	-	50	Co−Al_2O_3	18.7	250	1.5	14	24	118
Pd−Ag	Packed-bed	-	50	Co−Al_2O_3	18.7	400	1.5	94	27	118
Pd−Ag	Packed-bed	-	50	Co−Al_2O_3	18.7	400	3	100	90	119
Pd−Ag	Packed-bed	-	50	Co−Al_2O_3	18.7	400	1.5	100	30	119
Pd	Packed-bed	PSS	25	Co−Al_2O_3	3	400	4	90	20	35
Pd	Packed-bed	PSS	25	Co−Al_2O_3	3	400	8	100	50	35
Si−Al	Packed-bed	Al_2O3	3000	Na-CO/ZnO	3	350	1	50	-	120
Si−Al	Packed-bed	Al_2O_3	3000	Na-CO/ZnO	3	350	1	60	-	121
Pd−Cu	Packed-bed	Al_2O_3	3000	Na-CO/ZnO	3	350	1	70	-	121
Pd	Packed-bed	-	20	Co−Al_2O_3	13	400	12	82	12	122
Pd	Packed-bed	-	20	Ni/ZrO_2	13	400	12	87	8	122
Pd−Ag	Packed-bed	-	150	Pt−Co/$CeO_2ZrO_2Al_2O_3$	13	400	1.5	65	40	123
Pd−Ag	Packed-bed	-	150	Pt−Co/$CeO_2ZrO_2Al_2O_3$	13	490	3	90	65	123
Pd	Packed-bed	Al_2O_3	8	Ni/CeO_2	13	400	3	90	60	108
Pd	Packed-bed	Al_2O_3	8	Ni/CeO_2	3	400	3	95	65	108
Knudsen	Catalytic membrane reactor	PSS	-	Rh/SiO_2	5	450	-	100	-	124
Pt-Knudsen	Catalytic membrane reactor	PSS	-	Rh/SiO_2	5	500	-	100	-	124
Pd	Packed-bed	Ceramic	4.1	Ir/CeO_2	6	400	4	-	74	114
Pd	Packed-bed	Ceramic	4.1	Ir/CeO_2	6	600	13	-	95	114
Pd−Cu	Packed-bed	Ceramic	6.3	Ir/CeO_2	6	400	13	-	85	115
Pd−Cu	Packed-bed	Ceramic	6.3	Ir/CeO2	6	600	13	-	90	115
Pd	Packed-bed	-	1.3	Co−Na/ZnO	4	360	-	55	-	125
Pd−Cu	Packed-bed	-	2	Co−Na/ZnO	4	360	-	70	-	125
Pd	Packed-bed	Al_2O_3		Co−Pt/$CeO_2.ZrO_2.Al_2O_3$	6	400	2	60	50	109
Pd−Au−Pd−Au	Catalytic membrane reactor	PSS	20	Ni/Al_2O_3	5	500	5	100	-	110
Pd	Packed-bed	Al_2O_3		Pt−Ni/CeO_2	3	400	8	100	95	126
Pd−Ag	Packed-bed	-	30	Pd−Rh/CeO_2	6	650		100	55	127
Pd−Ag	Packed-bed	-	30	$Co_3[Si_2O_5]_2(OH)_2$	3	450	10	100	60	128
Pd−Ru	Packed-bed	-	50	Pd−Ru/DND	9	500	1	-	22	113
Pd−Ru	Packed-bed	-	50	Pt−Ru/DND	9	500	1	-	36	113
Pd−Ru	Packed-bed	-	50	Pt−Ni/DND	9	500	1	-	3	113
Pd−Ru−In	Packed-bed	-	50	Pd−Ru/DND	9	500	1	-	47	113
Knudsen	Catalytic membrane reactor	PSS	-	Rh/SiO_2	5	500	-	100	50	129
Knudsen	Catalytic membrane reactor	PSS	-	Rh/SiO_2−PT based	5	500	-	100	85	129
Pd−Ag	Catalytic membrane reactor	PSS	30	$[Co_2Mg_4Al_2(OH)_{16}]CO_3.4H_2O$	3	600	12	-	80	130
Pd−Ag	Packed-bed	-	150	Ru−Al_2O_3	13	400	1	50	2.2	131

which blocked active sites and hindered hydrogen permeation. Table 5 summarized the Pd alloys' MRs for hydrogen production.

5.2. Reforming Oxidation Processes. Partial oxidation (POX) and oxidative ethanol steam reforming (OSER), also known as autothermal reforming (ATR), have garnered attention due to the addition of oxygen, which helps prevent carbon deposition and the formation of ethylene and ethane during the reaction. These processes also offer faster response times and lower energy consumption compared to those of the ESR reaction. Both noble and non-noble catalysts, such as Ni, Pd, Pt, Ru, and Rh, have been studied for oxidative ethanol reforming.[22,31,132−134] The main reactions involved in ethanol POX are shown in eqs 9−12. Insufficient oxygen in the stream can result in incomplete partial oxidation, which is the preferred pathway.[22]

https://doi.org/10.1021/acs.energyfuels.4c02755
Energy Fuels 2024, 38, 19992−20014

Table 6. Summary Oxidative Ethanol Reaction in MR

Membrane	Support	Thickness (μm)	Catalyst	Oxygen to carbon	T (°C)	P (bar)	Ethanol conversion (%)	H_2 recovery (%)	Ref
Pd−Ag	-	150	Ru−Al_2O_3	1.3	400	2.5	100	15	131
Pd−Ag	-	150	Ru−Al_2O_3	0.6	400	2.5	40	28	131
Pd−Ag	PSS	-	Zn−Cu/Al_2O_3	0.2	300	9	65	-	138
Pd−Ag	PSS	-	Zn−Cu/Al_2O_3	0.2	450	3	82	-	138
Pd−Ag−Ni	PSS	-	MDC-3	0.2	350	5	69	-	140
Pd−Ag−Ni	PSS	-	MDC-3	02	450	5	78	-	140

$$C_2H_5OH + 0.5O_2 \leftrightarrow 2CO + 3H_2 \quad \Delta H^{\circ}_{298} = 57\ \text{kJ mol}^{-1} \tag{32}$$

$$C_2H_5OH + O_2 \leftrightarrow CO_2 + CO + 3H_2 \quad \Delta H^{\circ}_{298} = -226\ \text{kJ mol}^{-1} \tag{33}$$

$$C_2H_5OH + 1.5O_2 \leftrightarrow 2CO_2 + 3H_2 \quad \Delta H^{\circ}_{298} = -509\ \text{kJ mol}^{-1} \tag{34}$$

When oxygen content is sufficient, it leads to complete oxidation:[22]

$$C_2H_5OH + 3O_2 \leftrightarrow 2CO_2 + 3H_2O \quad \Delta H^{\circ}_{298} = -136\ \text{kJ mol}^{-1} \tag{35}$$

The OSER main reaction is[132]

$$C_2H_5OH + 1.8H_2O + 0.6O_2 \leftrightarrow 4.8H_2 + 2CO_2 \quad \Delta H^{\circ}_{298} = 4.4\ \text{kJ mol}^{-1} \tag{36}$$

POX and OSER reactions of ethanol for hydrogen production have primarily been studied in CRs, with limited research conducted in MRs. This is largely due to potential phase transitions in the catalyst active sites and the membrane, as excess oxygen can lead to oxidation.

5.2.1. Partial Oxidation Process (POX) in MRs. In the conventional partial oxidation process, ethanol is heated with a limited amount of pure oxygen in a reformer at high temperatures. The primary products of this reaction are CO and H_2, along with other gases such as nitrogen, carbon dioxide, water vapor, and minor byproducts. Similar to steam reforming, CO undergoes further conversion with steam in water−gas shift (WGS) reactors to produce additional H_2 and CO_2 in the presence of catalysts. Unlike steam reforming, partial oxidation is an exothermic and faster reaction, potentially leading to energy savings. However, POX is an expensive process due to the need for an air separation unit to supply pure oxygen. Despite the cost, POX has certain advantages over steam reforming including faster response times, compact design, and reduced sensitivity to fuel variations.

Research on POX in membrane reactors (MRs) has been limited, likely due to the negative impact of oxygen on membrane performance, which can lead to catalyst deactivation. Recently, Li et al. developed a novel ethanol reforming process that integrate oxygen separation, partial oxidation, and steam reforming in a MR using yttria-stabilized zirconia-$La_{0.8}Sr_{0.2}Cr_{0.5}Fe_{0.5}O_{3-\delta}$ as membrane and 5 wt % Ni−Ru/Al_2O_3 catalyst.[135] Their results demonstrated 99.9% ethanol conversion, 74.6% CO selectivity, and 90.8% H_2 selectivity at 800 °C with C_2H_5OH and steam feed rates of 30 and 54 mL/min, respectively. Additionally, Iulianeli et al. carried out ethanol POX in a dense Pd−Ag MR with Rh/Al_2O_3 catalyst to produce CO_x-free hydrogen.[136] In this case, complete ethanol conversion and more than 40% CO_x-free hydrogen recovery were achieved at T = 450 °C, sweep gas = 8.97 × 10^{-2} mol/h and GHSV = ∼1300 h^{-1}. When using a catalyst-free CMR, ethanol conversion decreased to 85% at 450 °C.

5.2.2. Oxidative Ethanol Steam Reforming (OESR) in MRs. Conventional autothermal reforming (ATR) combines steam reforming and partial oxidation within a single reformer. In this process, steam and oxygen are introduced simultaneously, allowing both reforming and oxidation reactions to occur at the same time. The exothermic partial oxidation reaction supplies the necessary heat for the endothermic steam reforming reaction, thereby lowering the overall energy requirements. Chen et al. conducted a literature review on oxidative ethanol steam reforming (OESR) in various reactor types, including fixed-bed reactors.[31]

In this regard, Iulianelli et al.[131] carried out ESR and oxidative ethanol steam reforming (OSER) in a Pd−Ag MR over a Ru−Al_2O_3 catalyst. The OSER reached 80% conversion at 400 °C, 1 bar, 2000 h^{-1}, and O_2/C_2H_5OH = 1.3, while ESR conversion was 50% at the same conditions using H_2O/C_2H_5OH = 13. Also, with the increase of oxygen, ethanol conversion decreased and reached 64% at an O_2/C_2H_5OH = 3.1. This decline could be due to the oxidation of both catalyst and membrane. Hydrogen yield and hydrogen recovery for both processes were low due to the low reaction pressure (1 bar)—hydrogen yield was 15% for ESR and 35% for OESR, while hydrogen recovery was 7.6% and 2.2% for OESR and ESR, respectively.[131] Lin et al.[137] investigated a Pd−Ag/PSS MR over a Zn−Cu catalyst for OESR. Results showed that ethanol conversion was 70% and 80% by using H_2O/C_2H_5OH = 3/1 and $H_2O/C_2H_5OH/O_2$ = 1/1/0.2, respectively, at 3 bar and 350 °C. Also, by increasing the temperature, conversion enhanced from 70% at 300 °C to 85% at 450 °C. In the following work, the OESR reaction performed in MR showed higher conversion than CR.[138] Santucci et al.[139] studied the influence of oxygen on the ESR reaction in the Pd−Ag MR with a Pt−Al_2O_3 catalyst. Data indicated that with the increase of feed flow rate, hydrogen yield decreased for both ESR and OESR at 450 °C and $H_2O/C_2H_5OH/O_2$ = 10/1/0.5. Also, the hydrogen yield improved with a slight increment of the C_2H_5OH/O_2 molar ratio from 0.2 to 0.7. The best result for hydrogen yield was obtained at 2 bar, 450 °C, and a molar ratio of $H_2O/C_2H_5OH/O_2$ = 10/1/0.5. Lin et al.[140] investigated the OESR reaction in the Pd−Ag/Ni-PSS membrane to examine the effects of oxygen. The results illustrated a similar ethanol conversion for the feed stream without and with oxygen content. For example, the conversions were 81% and 80% for the stream of $H_2O/C_2H_5OH/O_2$ = 1/3/0 and $H_2O/C_2H_5OH/O_2$ = 1/1/0.2, respectively. The reason for no improvement with oxygen

https://doi.org/10.1021/acs.energyfuels.4c02755
Energy Fuels 2024, 38, 19992−20014

Table 7. Modeling Details of Various MRs for Ethanol Reforming

MR type	Membrane	Modeling Dimension	Modeling software	Experimental data for model validation	Model−experimental error (%)	Temp (°C)	Pressure (bar)	Ethanol conversion (%)	Conclusion	Ref.
MR	Pd−Ag	1D	Modeling in Salford Plato3 FORTRAN95	Sahoo et al.[100]	5.8	400	8	MR − 95.3 CR − 44.5	MR can perform better than TR in terms of conversion and H_2 selectivities.	100
Membrane-microreactor	Pd−Ag	-	-	Papadias et al.[148]	-	-	-	-	A membrane exhibiting a 20-fold increase in hydrogen flux of experimental can generate enough hydrogen to achieve 72% efficiency targets	148
CMR	Pd−Ag	2D	Matlab programming environment	Espinal et al.[130]	-	700	2	100	Pure hydrogen production is augmented by elevating the operating temperature, pressure, and sweep ratio.	130
Monolithic catalyst−assisted MR	Ni−Cu alloy−Nd tungstate	1D	COMSOL	Eremeev et al.[88]	5−8	-	-	-	-	88
CMR	NiCu/$Nd_{5.5}WO_{11.25-\delta}$	1D	COMSOL	Bespalkl et al.;[157] Sadykov et al.[158]	<6	-	-	-	-	152
CMR	Pd-based	-	COMSOL	-	<6	600	-	[a]CMR - 93 [a]CR - 91	Reynolds numbers have effects on CMR performance	144
CMR	Pd/Au/Pd/Au	1D and 2D	Polymath and COMSOL	Ma et al.[110]	-	b	b	[b]100	-	110
CMR	Pd/Au/Pd/Au	2D	COMSOL	Ma et al.[153]	-	-	-	-	Counter-current sweep gas lowers the "cold spot", benefiting endothermic reactions.	153
CMR	Pd−Ag	-	Static and dynamic model	Hedayati et al.[154]	∼10−15	-	-	-	Simulation of the fuel flow rate change dynamics was more essential than the pressure change one.	154
Fluidized bed membrane reactor	Pd-based	-	-	Mas et al.[159]	-	677	3−20	100	A phenomenological model demonstrates the feasibility of achieving complete autothermal ESR	159
Fluidized bed Membrane reactor	Pd−Ag	-	-	Spallina et al.[156]	-	-	-	-	A model developed and used to design a small reactor system for domestic application	156
MR	Pd and Pd−Cu	1D	-	Yun et al.[125]	-	-	-	-	Increasing space velocity correlated with enhanced predicted conversion and hydrogen yield.	125
Membrane-assisted reactor	Pd−Ag	1D	Matlab (and AI-based)	Israni and Harold[160]	-	-	-	-	-	161

[a]The reported conversions are at a Reynolds number of 500 and S/E of 3. [b]The authors reported that the conversion of ethanol was 100% for every condition.

https://doi.org/10.1021/acs.energyfuels.4c02755
Energy Fuels 2024, 38, 19992−20014

could be due to the lower presence of steam in the stream with oxygen. Additionally, increasing pressure slightly decreased ethanol conversion, indicating that thermodynamic effects predominated over the shift effect in this scenario. Jin et al.[141] tested a $Ba_{0.5}Sr_{0.5}Co_{0.8}Fe_{0.2}O_{3-\delta}$ membrane mainly used for oxygen separation for ATR of ethanol for hydrogen production. They could produce 3.5 mol of H_2 per mol of ethanol at 750 °C. They showed that the MR was stable for 180 h under the ATR reforming conditions. Table 6 summarizes the oxidative ethanol steam reforming (OESR) reaction in MRs. The type of MR used is packed bed.

6. MODELING

Utilizing reactor modeling can help to predict the performance of the reactor and find optimized operating conditions.[142−145] Typically, models used to conduct simulations on MR are categorized into three groups: white box or theoretical models, black box or empirical models, and gray box or semiempirical models. Another method of classifying MR modeling is based on heterogeneous or pseudohomogeneous assumptions, which determine the complexity and precision of the model. A heterogeneous model treats the fluid and catalyst particles as two distinct phases and formulates balance equations for both. In contrast, a pseudohomogeneous model treats them as a single pseudophase and employs balance equations for only one phase.

Regarding dimensions (D), models for simulating a reaction in MR are classified into 1, 2, and 3D. 1D models consider the variation of properties in only one direction for a simple solution of their derivations, thus making it the most commonly used. 2D models consider hydrogen permeation and heat transfer through the membrane by incorporating radial concentrations and temperature gradients. This involves using radial profiles and employing a distinct differential volume for the two-dimensional simulation. Simulating an MR using 3D modeling is the most challenging approach, as it involves the entire geometry and considers angular direction profiles. However, their usage is constrained unless a nonsymmetrical reactor is utilized.[142]

Assumptions are generally made to generate the models; some are summarized in the following:

i. Steady-state conditions.
ii. Isothermal or nonisothermal conditions.
iii. Ideal gas behavior.
iv. A permeate side stream is considered a plug-flow with no axial dispersion and no pressure drop (1-D).
v. Infinite selectivity toward hydrogen permeation of a dense membrane with respect to other gases.
vi. The reaction occurs only at the catalyst surface.
vii. The steam effect on the membrane is negligible.
viii. The film transport resistance at the interface of gas/membrane is considered negligible.
ix. Pseudohomogenous condition in the reaction zone.
x. Physical properties, such as gas density, are constant with temperature.

Generally, a numerical model will be created to represent a system that is either isothermal or nonisothermal to simulate a reactor. Then, the model's validity will be confirmed by comparing its model data to experimental data in the scientific literature. For the model to predict the MR, confirming a strong correlation between its outcomes and the experimental data is crucial. Once validated, the model is employed to examine the influence of operating parameters, such as temperature, pressure, and GHSV, on the MR performance in terms of conversion, hydrogen yield, and recovery.

Continuously conducting process modeling of ESR is a crucial stage in designing, scaling up, and optimizing hydrogen production plants on the industrial scale.[146] Some studies related to ESR in Pd-based MRs have been reported and are summarized in Table 7. For the first time, Gallucci et al.[147] carried out simulation studies to investigate the performance of Pd−Ag MR compared to CR for ESR. They validated their model using the experimental results of Sahoo et al.[100] The best results were obtained at 400 °C and 8 bar, resulting in 95.3% ethanol conversion. The hydrogen production yield was 90%, and the hydrogen recovery was 94% under the same operating conditions. Papadias et al.[148] explored a mathematical model for ESR performance in a Pd−Ag microreactor and the conditions needed to approach distributed hydrogen production plants at higher pressures. The model used was validated by the experimental data. Their results showed that a membrane with flux at least 20 times higher than the one used for the experimental study would produce hydrogen yields that meet the hydrogen production plants.[148] Also, Koch et al.[149] developed a mathematical model for an ethanol reformer and implemented an adaptive and predictive control on a real-time system to take account of its nonlinear behavior. By utilizing this control, they reported that it is possible to decrease the response time of the reformer by a factor of 7, resulting in a response time of only 8 s. Zeynali et al.[150] employed a 2D computational fluid dynamic (CFD) model to study the performance of sorption-enhanced membrane reactors (SEMR) and MR during ESR. The findings from CFD modeling indicated that SEMR exhibited superior performance, achieving a roughly 20% enhancement in ethanol conversion (SEMR: 70% compared to MR: 59%).[150] Bobrova et al.[151] employed a 1D isothermal model to find a correlation between catalytic reactions and permeation phenomena within an MR for ESR over a monolithic catalyst. The MR operated under atmospheric pressure and at 700−900 °C. Their research findings indicate that employing a catalytic monolith within an MR can enhance hydrogen production and flux compared to CR.[151] Also, Bobrova et al.[152] implemented a 1D isothermal reaction−transport model to understand the fundamental interactions between catalytic and separation parts as they affect the performance of catalytic MRs for ESR using NiCu/Nd5.5WO11.25−δ as the dense layer. Their modeling results indicate that the asymmetric support contributes significantly, up to 70%, to the overall resistance across the membrane module. Additionally, the transport through the support was primarily governed by the layer's properties immediately adjacent to the permselective dense layer.[152] Chen et al.[144] developed a CFD model to examine the influence of the feed gas Reynolds number, reaction temperature, and S/C ratio on membrane performance in terms of ethanol conversion and hydrogen recovery. Their modeling results showed that the Pd membrane exhibited a superior performance in H2 permeation from the feed gas under low Reynolds numbers. However, the concentration polarization worsened, leading to a decline in H2 permeation. A low Reynolds number resulted in a prolonged residence time of H2 on the membrane, thereby enhancing the hydrogen recovery to 55.3%. Conversely, an increased Reynolds number led to incomplete ethanol conversion due to a shorter residence time.[144] Ma et al.[110] developed 1D and 2D CFD non-

https://doi.org/10.1021/acs.energyfuels.4c02755
Energy Fuels 2024, 38, 19992−20014

isothermal models using Polymath and COMSOL, respectively, to investigate the performance of a large-scale catalytic MR. The 2-D model outperformed the 1-D simulation, achieving a higher accuracy of 91% compared to the 85% accuracy of the 1-D model. The difference between the simulation results and the experiments was due to neglecting carbon deposition in the catalytic bed and temperature gradients along the catalytic bed.[110] As a follow-up, Ma et al.[153] developed a 2D nonisothermal CFD model based on the previously experimentally validated isothermal model to study the heat and mass transfer phenomenon in the large-scale catalytic membrane reactor (CMR). According to their findings, the model revealed a temperature gradient along the reactor, indicating a "cold spot" at the inlet area, which is unfavorable to the endothermic ESR process. By altering the sweep gas to counter-current, the "cold spot" size diminishes.[153] Hedayati et al.[154] presented a simpler simulation methodology for examining the dynamics of pure hydrogen production rate by CMR under transient conditions, using principles in the Arrhenius' model, mass balance, ideal gas, and Sieverts' law. They developed a static model based on Arrhenius' law for the catalytic zone to compute the total molar production rates of ESR products alongside a dynamic model under the ideal gas law to simulate the dynamics of pure H2 production rate in scenarios involving adjustments in pressure set points or feed flow rates. Simulation outcomes indicated that the dynamics of feed flow rate change were more critical than those of pressure change, as the system exhibited significantly faster responses to such adjustments.[154] Siadi et al.[146] reported the effects of different designs and operational conditions on ethanol conversion, hydrogen recovery, and total hydrogen yield by utilizing a 2D nonisothermal stationary mathematical model applied to CMR. A thermal analysis was also conducted to predict the temperature profiles. The model predictions showed that elevated temperature, pressure, and sweep gas ratio enhanced pure hydrogen production. Additionally, the thermal analysis demonstrated that during the initial stages of CMR operation, characterized by high inlet concentrations of reactants, the rapid reaction rate of ESR controlled temperature variation, resulting in a temperature decrease. Subsequently, the temperature reached a minimum value before gradually increasing when the reactor dimensionless length was approximately 0.2.[146] Gallucci et al.[155] developed a model to study the possibility of performing autothermal reforming without adding oxygen/air to the reaction zone of a fluidized bed membrane reactor (FBMR). The model assumed that the reactor consisted of bubble and emulsion phases. The simulation results of the two-phase model indicated the potential for recovering pure hydrogen via Pd-based membranes, achieving complete ethanol conversion while fulfilling the heat requirements for the reforming reaction through the combustion of approximately 15% of the recovered hydrogen, thereby achieving overall ATR.[155] Furthermore, Spallina et al.[156] formulated and used a two-phase model to design a compact FBMR intended for domestic application. The findings indicated that a membrane area of 0.45 m2 was necessary to generate H2 for a 5 kWe PEM fuel cell-based micro-CHP system. The modeling additionally demonstrated that an approximate amount of 250 g of catalyst was needed to obtain the necessary conversion, given a total of 7 kg of solid material required for reactor filling.[156] Yun et al.[125] developed a 1D model for the ESR in Pd and Pd−Cu MRs using a simplified power law. They reported that the observed rise in predicted conversion and hydrogen yield enhancement with increasing space velocity can be explained by the different ethanol partial pressures in the MRs and the CR.[125] Table 7 summarizes the modeling works using MRs used for ESR.

7. TECHNOECONOMIC ANALYSIS AND LIFE CYCLE ASSESSMENT

Different research studies have shown the feasibility and advantage of using MR over CR. However, no review articles discussed the hydrogen production cost from ESR in MR and CR. To understand the feasibility of scaling up ESR in MR to the industrial level, techno-economical and life cycle assessments are needed. In this regard, Wang et al.[162] investigated hydrogen production via ESR in a Pd MR. The energy source for the reaction was assumed to be provided by solar or wind power. They found that the cost of 1 kg of H_2 was equal to 4.16$, while in a study by Khamhaeng et al.,[163] the cost of hydrogen production was calculated 1.58$ in a CR. The cost difference can be attributed to various factors, such as the utilization of Pd membrane for hydrogen separation, the choice of solar or wind as feedstock for energy production, variation in methodology, and the volume of hydrogen production. Table 8 shows and compares different methods for hydrogen production. As can be seen, the cost of hydrogen production from ESR is lower than that of methanol steam reforming (MSR), but higher than that of SMR. The reasons could be due to different prices in feedstock, different methodologies, and production volume. However, by comparing the cost of hydrogen production by the ESR in the MR with electrolysis, it can be observed that the ESR in the MR has a lower hydrogen production cost than electrolysis techniques.

Table 8. Hydrogen Production Cost with Different Routes[9,13,62,163,164]

Process	Feedstock	Energy source	Hydrogen cost ($/kg)
SMR without CCS	Natural gas	Fossil fuel	1.26
SMR with CCS	Natural gas	Fossil fuel	1.88
SMR with MR	Natural gas	Fossil fuel	3.54
ESR with MR	**Ethanol**	**Solar-wind**	**4.16**
ESR in CR	**Ethanol**	**Ethanol**	**1.58**
MSR with MR	Methanol	Synthetic fuel	6.43−8.82
Coal gasification (CG) without CCS	Coal	Fossil fuel	1.34
CG with CCS	Coal	Fossil fuel	1.63
ATR of methane with CCS	Natural gas	Fossil fuel	1.48
Biomass gasification	Woody biomass	Generated steam	1.77−2.05
Biomass pyrolysis	Woody biomass	Generated steam	1.25−2.2
Methane pyrolysis	Natural gas	Generated steam	1.59−1.7
Solar PV electrolysis	Water	Solar	5.78−23.27
Solar thermal electrolysis	Water	Solar	5.1−10.49
Photoelectrolysis	Water	Solar	10.36
Solar thermolysis	Water	Solar	7.98−8.4
Wind electrolysis	Water	Wind	5.89−6.03

Evaluating the life cycle assessment (LCA) is essential to determine CO_2 emissions per kilogram of hydrogen produced during the ESR process. While no studies have specifically examined the LCA for ESR in MRs, it can be approximated by

https://doi.org/10.1021/acs.energyfuels.4c02755
Energy Fuels 2024, 38, 19992−20014

assessing the process in CRs. Table 9 presents a comparative analysis of various hydrogen production processes from different feedstocks, emphasizing their CO_2 emissions in kilograms per kilogram of hydrogen produced. Bioethanol stands out as a lower-emission option compared with fossil-based sources. For example, in the study by Susmozas et al.,[165] bioethanol steam reforming produces 3.79 kg_{CO2} per kg_{H2}, significantly lower than glycerol steam reforming, which emits 12.6 kg_{CO2}, and methane steam reforming at 13 kg_{CO2} as reported by Khila et al.[166] Even in autothermal reforming, bioethanol emits 7 kg_{CO2} per kg_{H2}, still outperforming fossil fuels like methane. Similarly, in Siddiqui and Dincer's study,[167] ethanol steam reforming produces 10 kg_{CO2} per kg_{H2}, which is lower than methane at 14 kg_{CO2} and methanol at 16 kg_{CO2}. Biomass gasification in this study results in just 4 kg_{CO2}, further illustrating that biomass-derived ethanol (bioethanol) offers a substantial reduction in emissions compared to coal gasification, which emits 22 kg_{CO2}, and water electrolysis using grid electricity, which generates 26 kg_{CO2}. In Cetinkaya's study,[168] water electrolysis using renewable energy sources like wind or solar power shows the lowest emissions, ranging from 1 to 2 kg_{CO2} per kg_{H2}, but these processes depend heavily on the availability of sustainable energy. Bioethanol, on the other hand, provides a more feasible low-carbon alternative in regions with limited access to renewable energy. So far, no research study has investigated the life cycle assessment (LCA) of hydrogen production via the ESR in MRs. However, using MRs could further reduce CO_2 emissions compared to conventional reactors (CRs) because MRs operate at lower temperatures and pressures, with CO_2 being captured at the membrane downstream outlet. Additionally, MRs require fewer accessories (e.g., pumps and compressors), which reduce both the process cost and energy demand. The overall benefits of bioethanol include lower CO_2 emissions compared to fossil fuels, their renewable nature contributing to a closed carbon cycle, and their potential for high hydrogen yield. In summary, bioethanol emerges as a sustainable, lower-emission alternative to traditional fossil fuels for hydrogen production, while water electrolysis with renewable energy remains the cleanest option but is less accessible in all regions.

Table 9. Summary of CO_2 Emission in Different Routes of Hydrogen Production

Research Study	Feedstock	Process	CO_2 emission (kg_{CO2}/kg_{H2})	Reference
Susmozas et al.	**Bioethanol**	**Steam reforming**	**3.79**	165
	Glycerol	Steam reforming	12.6	165
Khila et al	Methane	Steam reforming	13	166
	Bioethanol	**Auto thermal reforming**	7	166
	Biomass	Gasification	4	166
	Water	Water electrolysis - Nuclear	2	166
	Water	Water electrolysis - Solar	2	166
Siddiqui and Dincer	Methane	Steam reforming	14	167
	Methanol	Steam reforming	16	167
	Ethanol	**Steam reforming**	**10**	167
	Biomass	Gasification	4	167
	Coal	Gasification	22	167
	Water	Water electrolysis - Grid	26	167
Cetinkaya	Methane	Steam reforming	12	168
	Coal	gasification	11	168
	Water	Water electrolysis - wind	1	168
	Water	Water electrolysis - solar	2	168

8. CHALLENGES AND FUTURE TRENDS

(1) Most studies have investigated supported and unsupported pure Pd or Pd−Ag MR for performing ESR reaction with various catalysts. However, it has been reported that some binary and ternary Pd alloy membranes have demonstrated better chemical and physical stability alongside appropriate hydrogen permeation.[46,169] For instance, Pd−Au and Pd−Cu membranes exhibited greater chemical and physical stability compared to that of Pd−Ag membranes, suggesting their potential for future ESR applications. Furthermore, some ternary alloys such as Pd−Ag−Au, Pd−Ag−Cu, and Pd−Ag−Y have shown high chemical and physical stability and higher hydrogen permeation compared to that of binary ones.[170,171] Ternary Pd alloy membranes could therefore offer a promising alternative for future ESR applications. Consequently, selecting suitable Pd alloy membranes could effectively address challenges related to chemical and physical stability under reaction conditions.

(2) An additional challenge that needs to be addressed in future work is the long-term stability of Pd-based MRs for the ESR reaction. To date, most studies have focused on the performance of MRs in terms of conversion efficiency, hydrogen recovery, production, and yield. However, for the successful scale-up of MRs to industrial applications, long-term stability is a critical factor. Therefore, future research should prioritize investigating the long-term stability of Pd alloy MRs in ESR processes.

(3) The increasing cost of manufacturing, driven by the rise in price of Pd in recent years, poses a challenge to the advancement of this technology. Hence, it is crucial to reduce membrane thickness, although excessively thin Pd layers can lead to various issues, such as pinhole formation, metallic interdiffusion between membrane and support, different thermal expansion of membrane and support, and low mechanical stability of the membrane under high operating pressure within a reaction environment.[45,169,172] Future efforts should focus on improving the deposition techniques of Pd alloy membranes onto supports to mitigate defects, select suitable support materials, and ensure better adhesion between membrane and support.

(4) Additionally, more research efforts should be directed toward more cost-effective H_2-selective membranes, such as those made from polymeric, non-noble metals, zeolites, and ceramics, for ethanol reforming in MRs. Polymeric membranes are capable of withstanding high-pressure drops and are cost-effective.[173] However, their operating temperature is below 200 °C,[174] which is very low for ethanol reforming. Incorporating additives and employing cross-linking methods can enhance the thermal stability of polymeric membranes. Although it appears unattainable, developing heat-resistant polymeric membranes capable of withstanding temperatures

https://doi.org/10.1021/acs.energyfuels.4c02755
Energy Fuels 2024, 38, 19992−20014

up to 1000 °C will renovate H_2 production via ethanol reforming in MRs. Zeolite membranes are thermally and chemically stable for H_2 separation.[67] However, these membranes are brittle and challenging to produce. Also, the high production costs associated with ceramic membranes pose a significant barrier to their commercial-scale utilization.[67] Ni-based membrane is superior to Pd due to cost and ability to resist the poisoning effect of CO and sulfur at high temperatures. However, Ni membranes exhibit a lower H_2 permeability than Pd-based membranes. Strategic ways to improve H_2 separation of Ni membranes include reduction of membrane thickness and increase of membrane surface per unit volume ratio (by adopting hollow fiber geometry).[85,175] More advanced research on the emerging membranes could provide solutions to the current challenges associated with MRs.

(5) Another challenge in the advancement of hydrogen production from bioethanol in MRs involves the presence of impurities in the feed. These impurities range from heavy and complex hydrocarbons to the presence of sulfur and phosphorus in the bioethanol. The presence of heavy and complex hydrocarbons could result in coke formation on both catalysts and membranes, as well as induce side reactions that negatively impact the MR performance by reducing conversion, hydrogen recovery, and yield.[176] Additionally, the presence of sulfur poisons the catalyst and could block the active sites for hydrogen permeation on the Pd alloy membrane.[109] Moreover, the presence of sulfur leads to the formation of the Pd−S phase, adversely affecting hydrogen permeation and selectivity. Consequently, purifying bioethanol from any impurities before employing ESR in MR is essential to optimize performance and prevent catalyst and membrane degradation.[109]

(6) Modeling has been a powerful tool in studying and predicting the performance of MR for hydrogen production. Authors commonly reported that their models reasonably agreed with the experimental data upon validation and following modeling assumptions to simplify physical problems. Some of these assumptions tend to model physical systems in ideal conditions, deviating from real behaviors. For instance, some studies[125,144] assume that the permselectivity of membranes to hydrogen is infinite and zero for other gases. This assumption is not always valid for membranes in real applications. Future works on modeling should incorporate fewer assumptions to ensure that MRs are modeled under real conditions.

(7) Modeling has been a powerful tool in studying and predicting the performance of MR for hydrogen production. There is always associated discrepancies between the model prediction and experimental data during validation. The discrepancies might be stemmed from either the experimental measurements or model itself. The error from modeling might be from assumptions, kinetic rate expressions, or the solution method.[161] It is commonly reported by authors that their models reasonably agree with the experimental data upon validation and modeling assumptions are made to simplify physical problems. Some of these assumptions tend to model physical systems in ideal conditions, deviating from real behaviors. For instance, some studies[125,144] assume that the permselectivity of membranes to hydrogen is infinite and zero for other gases. This assumption is not always valid for membranes in real applications. Future works on modeling should incorporate fewer assumptions to ensure that MRs are modeled under real conditions. Misappropriation of boundary conditions and initial conditions is also likely to result in huge error between model and experimental data. Implementation of sensitivity analysis to understand how these conditions affect the model's outcome could minimize the error. Similar to the approach of Dehdashtijahromi et al.[177] and Bakhtyari et al.,[161] future modeling should be conducted with exergy and sensitivity analysis to enhance the understanding of process efficiency, sustainability and impact of the operating conditions in ESR. Typically, models are developed to address specific scenarios and this may limit the model application to broader contexts such as for industrial use. For MR scaling up to industrial level, future computational research on ESR should incorporate diverse environmental factors. Additionally, the simplifications and approximations in model assumptions should be refined to ensure their applicability in industrial H_2 production. Given the increasing influence of artificial intelligence (AI), researchers should prioritize the development of AI models and hybrid models—integrating conventional models with AI approaches—for the prediction of ESR in MR.

(8) To the best of our knowledge, there is only one study on techno-economical analysis (TEA) and no study on life cycle assessment (LCA) of hydrogen production through ESR in Pd MR. TEA and LCA could provide important information such as the cost of hydrogen production, required energy, and CO_2 emission. Thus, future research efforts should focus on providing outcomes regarding TEA and LCA because of the necessity of scaling up this process to the industrial level.

9. CONCLUSION

Hydrogen has shown excellent potential for substituting fossil fuels, particularly natural gas, for the industrial and residential sectors. However, hydrogen is mainly obtained by fossil fuel processes, which is not a sustainable pathway for the future. On the other hand, hydrogen could be obtained from alcohols and biofeedstock to lower CO_2 emissions to the atmosphere. Ethanol and bioethanol could be obtained from biomass and used for renewable hydrogen production. Ethanol steam reforming in MRs gained attention because it operates at lower operating conditions and has higher conversion, lower cost, and lower carbon footprint than the SMR. In addition, the MR could produce hydrogen from ethanol in decentralized units where ethanol is made available, reducing the cost of transportation. Among MRs, Pd alloy membranes are mostly used for ESR reactions due to their complete selectivity toward hydrogen permeation. The MR utilization and the oxygen addition to the ESR reaction could further inhibit the undesirable side reactions and decrease carbonaceous material formation reactions, leading to higher yields, conversions, and stability. The experimental research showed that MR's ESR is favored at high temperature, pressure, S/C ratio, and low flow

https://doi.org/10.1021/acs.energyfuels.4c02755
Energy Fuels 2024, 38, 19992−20014

rate. The performance of MRs for ESR under different operating conditions has been successfully investigated by using mathematical modeling and simulations. These investigations have not only shed light on the behavior of Pd-based MRs but also provided valuable insights into their performance under different scenarios. Importantly, modeling serves as an indispensable tool for predicting performance and scaling up MRs for hydrogen production, offering a pathway toward the efficient and sustainable utilization of this technology on an industrial scale.

AUTHOR INFORMATION

Corresponding Author

Simona Liguori − *Chemical and Biomolecular Engineering Department, Clarkson University, Potsdam, New York 13699, United States;* orcid.org/0000-0001-9061-0475; Email: sliguori@clarkson.edu

Authors

Omid Jazani − *Chemical and Biomolecular Engineering Department, Clarkson University, Potsdam, New York 13699, United States*

Moses Adejumo − *Chemical and Biomolecular Engineering Department, Clarkson University, Potsdam, New York 13699, United States*

Mohamed A. Elharati − *Chemical and Biomolecular Engineering Department, Clarkson University, Potsdam, New York 13699, United States*

Complete contact information is available at: https://pubs.acs.org/10.1021/acs.energyfuels.4c02755

Notes

The authors declare no competing financial interest.

Biographies

Omid Jazani is a Ph.D candidate in the Chemical and Biomolecular Engineering Department at Clarkson University. He obtained his M.Sc and B.Sc in Chemical Engineering from Science and Research Azad University. His research area focus on synthesis of Pd-based membrane for hydrogen production and separation, reforming reactions, and carbon capture and utilization.

Moses Adejumo is a doctoral candidate in the Chemical and Biomolecular Engineering Department of Clarkson University. He earned his bachelor's degree in Chemical Engineering from Obafemi Awolowo University, Nigeria, in 2017. His current research focuses on the synthesis and characterization of molten salt (IMS) membranes for ammonia separation and modeling of ammonia through molten salt membranes.

Dr. Mohamed Ali Elharati received his BSc and MSc degrees in Chemical Engineering from the University ofTripoli, Libya, and Stellenbosch University, South Africa. Dr. Elharati completed his Ph.D. in Chemical and Biochemical Engineering at Washington State University in 2022. He joined Clarkson University as a Postdoctoral Research Associate in the Chemical and Biomolecular Engineering Department in 2023. Dr. Elharati's research area focuses on heterogeneous catalysis, CO_2 capture, hydrogen fuel, and membrane separation technology.

Dr. Simona Liguori is an assistant professor at Clarkson University. She received her master's degree and Ph.D. in Chemical Engineering from the University of Calabria, Italy. Dr. Liguori's research efforts are devoted to developing processes and materials that play pivotal roles in energy conversion with enhanced efficiency and environmental sustainability. In particular, her objective is to create and develop clean hydrogen and cost-effective technologies to be beneficial for society and economic growth, while reducing the environmental impact.

ABBREVIATIONS

ATR: auto thermal reforming
CCS: carbon capture and sequestration
CCUS: carbon capture, utilization, and sequestration
CFD: computational fluid dynamic
CG: coal gasification
CMR: catalytic membrane reactor
CR: conventional reactor
D: dimension
ELP: Electroless plating
ESR: ethanol steam reforming
FBMR: fluidized bed membrane reactors
GHGs: greenhouse gases
GHSV: gas hourly space velocity
IPCC: intergovernmental panel on climate change
MR: membrane reactor
MSR: methanol steam reforming
OESR: oxidative ethanol steam reforming
PBMR: packed bed membrane reactors
PEMFCs: proton exchange membrane fuel cells
PSA: pressure swing adsorption
PSS: porous stainless steel
R: universal gas constant
SMR: steam methane reforming
WGS: water gas shift
WHSV: weight hourly space velocity

Symbols

α: ideal selectivity
δ: membrane thickness
dp: pore size
E_a: apparent activation energy
Pe_{H2}: hydrogen permeability
$p^n_{H2,retentate}$: partial pressure in the retentate side
$p^n_{H2,permeate}$: partial pressures in the permeate side
Pe^0: pre-exponential factor
P_{H2}: hydrogen permeance
J_{H2}: hydrogen permeating flux

REFERENCES

(1) Osman, A. I.; Mehta, N.; Elgarahy, A. M.; Hefny, M.; Al-Hinai, A.; Al-Muhtaseb, A. H.; Rooney, D. W. Hydrogen Production, Storage, Utilisation and Environmental Impacts: A Review. *Environmental Chemistry Letters* **2022**, *20*, 153−188.

(2) Ishaq, H.; Dincer, I.; Crawford, C. A Review on Hydrogen Production and Utilization: Challenges and Opportunities. *Int. J. Hydrogen Energy* **2022**, *47* (62), 26238−26264.

(3) Younas, M.; Shafique, S.; Hafeez, A.; Javed, F.; Rehman, F. An Overview of Hydrogen Production: Current Status, Potential, and Challenges. *Fuel.* **2022**, *316*, 123317.

(4) Abdalla, A. M.; Hossain, S.; Nisfindy, O. B.; Azad, A. T.; Dawood, M.; Azad, A. K. Hydrogen Production, Storage, Transportation and Key Challenges with Applications: A Review. *Energy Conversion and Management* **2018**, *165*, 602−627.

(5) IEA. *CO_2 Emissions in 2022*; Paris, 2022.

(6) IEA. *Key World Energy Statistics 2021*; Paris, 2021.

(7) Ji, M.; Wang, J. Review and Comparison of Various Hydrogen Production Methods Based on Costs and Life Cycle Impact Assessment Indicators. *International Journal of Hydrogen Energy.* **2021**, *46*, 38612−38635.

(8) Allen, M.; Dube, O.P.; Solecki, W.; Aragón-Durand, F.; Cramer, W.; Humphreys, S.; Kainuma, M.; Kala, N. M. J.; Mulugetta, Y.; Perez, R.; Wairiu, M.; Zickfeld, K. Framing and Context. In *Global Warming of 1.5 °C*, An IPCC Special Report on the Impacts of Global Warming of 1.5 °C above Pre-Industrial Levels and Related Global Greenhouse Gas Emission Pathways, in the Context of Strengthening the Global Response to the Threat of Climate Change, Sustainable Development, and Efforts to Eradicate Poverty; IPCC, 2018.
(9) Jazani, O.; Bennett, J.; Liguori, S. Carbon-Low, Renewable Hydrogen Production from Methanol Steam Reforming in Membrane Reactors − a Review. *Chemical Engineering and Processing - Process Intensification* **2023**, *189*, No. 109382.
(10) Dawood, F.; Anda, M.; Shafiullah, G. M. Hydrogen Production for Energy: An Overview. *International Journal of Hydrogen Energy.* **2020**, *45*, 3847−3869.
(11) Martinez-Burgos, W. J.; de Souza Candeo, E.; Pedroni Medeiros, A. B.; Cesar de Carvalho, J.; Oliveira de Andrade Tanobe, V.; Soccol, C. R.; Sydney, E. B. Hydrogen: Current Advances and Patented Technologies of Its Renewable Production. *Journal of Cleaner Production.* **2021**, *286*, 124970.
(12) Bahrami, A.; Soltanifar, F.; Fallahi, P.; Meschi, S. S.; Sohani, A. Energy and Economic Advantages of Using Solar Stills for Renewable Energy-Based Multi-Generation of Power and Hydrogen for Residential Buildings. *Buildings* **2024**, *14* (4), 1041.
(13) Zhang, B.; Zhang, S. X.; Yao, R.; Wu, Y. H.; Qiu, J. S. Progress and Prospects of Hydrogen Production: Opportunities and Challenges. *Journal of Electronic Science and Technology* **2021**, *19* (2), 100080.
(14) Ferraren-De Cagalitan, D. D. T.; Abundo, M. L. S. A Review of Biohydrogen Production Technology for Application towards Hydrogen Fuel Cells. *Renewable and Sustainable Energy Reviews.* **2021**, *151*, 111413.
(15) Jazani, O.; Bennett, J.; Liguori, S. Effect of Temperature, Air Exposure and Gas Mixture on Pd82−Ag15−Y3Membrane for Hydrogen Separation. *Int. J. Hydrogen Energy* **2024**, *51*, 624.
(16) Martino, M.; Ruocco, C.; Meloni, E.; Pullumbi, P.; Palma, V. Main Hydrogen Production Processes: An Overview. *Catalysts.* **2021**, *11*, 547.
(17) Office of Fossil Fuels-United States Department of Energy. *Hydrogen Strategy Enabling A Low-Carbon Economy*; Washington, DC, 2020.
(18) Chen, L.; Qi, Z.; Zhang, S.; Su, J.; Somorjai, G. A. Catalytic Hydrogen Production from Methane: A Review on Recent Progress and Prospect. *Catalysts* **2020**, *10* (8), 858.
(19) Liguori, S.; Kian, K.; Buggy, N.; Anzelmo, B. H.; Wilcox, J. Opportunities and Challenges of Low-Carbon Hydrogen via Metallic Membranes. *Prog. Energy Combust. Sci.* **2020**, *80*, No. 100851.
(20) Shtyka, O.; Dimitrova, Z.; Ciesielski, R.; Kedziora, A.; Mitukiewicz, G.; Leyko, J.; Maniukewicz, W.; Czylkowska, A.; Maniecki, T. Steam Reforming of Ethanol for Hydrogen Production: Influence of Catalyst Composition (Ni/Al2O3, Ni/Al2O3−CeO2, Ni/Al2O3−ZnO) and Process Conditions. *Reaction Kinetics, Mechanisms and Catalysis* **2021**, *132* (2), 907−919.
(21) Özkan, G.; Şahbudak, B.; Özkan, G. Effect of Molar Ratio of Water/Ethanol on Hydrogen Selectivity in Catalytic Production of Hydrogen Using Steam Reforming of Ethanol. *Int. J. Hydrogen Energy* **2019**, *44* (20), 9823−9829.
(22) Rabenstein, G.; Hacker, V. Hydrogen for Fuel Cells from Ethanol by Steam-Reforming, Partial-Oxidation and Combined Auto-Thermal Reforming: A Thermodynamic Analysis. *J. Power Sources* **2008**, *185* (2), 1293−1304.
(23) Kugai, J.; Velu, S.; Song, C. Low-Temperature Reforming of Ethanol over CeO2-Supported Ni-Rh Bimetallic Catalysts for Hydrogen Production. *Catal. Lett.* **2005**, *101* (3), 255−264.
(24) Chen, W.-H.; Lu, C.-Y.; Tran, K.-Q.; Lin, Y.-L.; Naqvi, S. R. A New Design of Catalytic Tube Reactor for Hydrogen Production from Ethanol Steam Reforming. *Fuel* **2020**, *281*, No. 118746.
(25) Chen, W.-H.; Biswas, P. P.; Ubando, A. T.; Park, Y.-K.; Ashokkumar, V.; Chang, J.-S. Design of Experiment for Hydrogen Production from Ethanol Reforming: A State-of-the-Art Review. *Fuel* **2023**, *342*, No. 127871.
(26) Deng, Y.; Li, S.; Appels, L.; Zhang, H.; Sweygers, N.; Baeyens, J.; Dewil, R. Steam Reforming of Ethanol by Non-Noble Metal Catalysts. *Renewable and Sustainable Energy Reviews* **2023**, *175*, No. 113184.
(27) Meng, H.; Zhang, J.; Yang, Y. Recent Status in Catalyst Modification Strategies for Hydrogen Production from Ethanol Steam Reforming. *ChemCatChem.* **2023**, *15* (17), No. e202300733.
(28) Gasparetto, H.; Salau, N. P. G. A Review on Ethanol Steam Reforming Focusing on Yttria-Stabilized Zirconia Catalysts: A Look into Hydrogen Production for Fuel Cells. *Fuel* **2024**, *371*, No. 132140.
(29) Iulianelli, A.; Basile, A. Green Hydrogen Production from Biocompounds through Membrane Engineering. In *Current Trends and Future Developments on (Bio-) Membranes*; Elsevier, 2020; pp 21−41. DOI: 10.1016/b978-0-12-817384-8.00002-9.
(30) Iulianelli, A.; Dalena, F.; Basile, A. H2 Production from Bioalcohols and Biomethane Steam Reforming in Membrane Reactors. In *Bioenergy Systems for the Future: Prospects for Biofuels and Biohydrogen*; Elsevier Inc., 2017; pp 321−344. DOI: 10.1016/B978-0-08-101031-0.00009-0.
(31) Chen, W. H.; Biswas, P. P.; Ong, H. C.; Hoang, A. T.; Nguyen, T. B.; Dong, C. Di. A Critical and Systematic Review of Sustainable Hydrogen Production from Ethanol/Bioethanol: Steam Reforming, Partial Oxidation, and Autothermal Reforming. *Fuel* **2023**, *333*, 126526.
(32) Full, J.; Geller, M.; Ziehn, S.; Schließ, T.; Miehe, R.; Sauer, A. Carbon-Negative Hydrogen Production (HyBECCS): An Exemplary Techno-Economic and Environmental Assessment. *Int. J. Hydrogen Energy* **2024**, *52*, 594−609.
(33) Rosa, L.; Mazzotti, M. Potential for Hydrogen Production from Sustainable Biomass with Carbon Capture and Storage. *Renewable and Sustainable Energy Reviews* **2022**, *157*, No. 112123.
(34) Basile, A.; Gallucci, F.; Paturzo, L. A Dense Pd/Ag Membrane Reactor for Methanol Steam Reforming: Experimental Study. *In Catalysis Today* **2005**, *104*, 244−250.
(35) Basile, A.; Pinacci, P.; Iulianelli, A.; Broglia, M.; Drago, F.; Liguori, S.; Longo, T.; Calabro, V. Ethanol Steam Reforming Reaction in a Porous Stainless Steel Supported Palladium Membrane Reactor. *Int. J. Hydrogen Energy* **2011**, *36* (3), 2029−2037.
(36) Chang, A. C. C.; Lin, W. H.; Lin, K. H.; Hsiao, C. H.; Chen, H. H.; Chang, H. F. Reforming of Glycerol for Producing Hydrogen in a Pd/Ag Membrane Reactor. *Int. J. Hydrogen Energy* **2012**, *37* (17), 13110−13117.
(37) Iulianelli, A.; Dalena, F.; Liguori, S.; Calabrò, V.; Basile, A. Membrane Reactors for Steam Reforming of Glycerol and Acetic Acid to Produce Hydrogen. In *Membrane Reactors for Energy Applications and Basic Chemical Production*; Elsevier Inc., 2015; pp 249−266. DOI: 10.1016/B978-1-78242-223-5.00008-X.
(38) Adejumo, M.; Jazani, O.; Shildebayev, T.; Liguori, S. Chapter Four - Efficient Ammonia Decomposition in Membrane Reactor for Hydrogen Separation, Purification, Storage, and Utilization. In *Progresses in Ammonia: Science, Technology and Membranes*; Basile, A., Rahimpour, M. R., Eds.; Elsevier, 2024; pp 67−94. DOI: 10.1016/B978-0-323-88503-4.00002-8.
(39) Iulianelli, A.; Liguori, S.; Huang, Y.; Basile, A. Model Biogas Steam Reforming in a Thin Pd-Supported Membrane Reactor to Generate Clean Hydrogen for Fuel Cells. *J. Power Sources* **2015**, *273*, 25−32.
(40) Amiri, T. Y.; Ghasemzageh, K.; Iulianelli, A. Membrane Reactors for Sustainable Hydrogen Production through Steam Reforming of Hydrocarbons: A Review. *Chemical Engineering and Processing - Process Intensification* **2020**, *157*, 108148.
(41) Basile, A.; Iulianelli, A.; Longo, T.; Liguori, S.; De Falco, M. Pd-Based Selective Membrane State-of-the-Art. In *Membrane Reactors for Hydrogen Production Processes*; De Falco, M., Marrelli, L., Iaquaniello, G., Eds.; Springer London: London, 2011; pp 21−55. DOI: 10.1007/978-0-85729-151-6_2.

(42) Binazadeh, M.; Mamivand, S.; Sohrabi, R.; Taghvaei, H.; Iulianelli, A. Membrane Reactors for Hydrogen Generation: From Single Stage to Integrated Systems. *Int. J. Hydrogen Energy* **2023**, *48* (99), 39225−39253.
(43) Arratibel Plazaola, A.; Pacheco Tanaka, D. A.; Van Sint Annaland, M.; Gallucci, F. Recent Advances in Pd-Based Membranes for Membrane Reactors. *Molecules (Basel, Switzerland)*. **2017**, *22*, 51.
(44) Habib, M. A.; Harale, A.; Paglieri, S.; Alrashed, F. S.; Al-Sayoud, A.; Rao, M. V.; Nemitallah, M. A.; Hossain, S.; Hussien, M.; Ali, A.; Haque, M. A.; Abuelyamen, A.; Shakeel, M. R.; Mokheimer, E. M. A.; Ben-Mansour, R. Palladium-Alloy Membrane Reactors for Fuel Reforming and Hydrogen Production: A Review. *Energy and Fuels.* **2021**, *35*, 5558−5593.
(45) Alique, D.; Martinez-Diaz, D.; Sanz, R.; Calles, J. A. Review of Supported Pd-Based Membranes Preparation by Electroless Plating for Ultra-Pure Hydrogen Production. *Membranes.* **2018**, *8*, 5.
(46) Conde, J. J.; Maroño, M.; Sánchez-Hervás, J. M. Pd-Based Membranes for Hydrogen Separation: Review of Alloying Elements and Their Influence on Membrane Properties. *Separation and Purification Reviews* **2017**, *46*, 152−177.
(47) Mamivand, S.; Binazadeh, M.; Sohrabi, R. Applicability of Membrane Reactor Technology in Industrial Hydrogen Producing Reactions: Current Effort and Future Directions. *Journal of Industrial and Engineering Chemistry* **2021**, *104*, 212−230.
(48) Ogo, S.; Sekine, Y. Recent Progress in Ethanol Steam Reforming Using Non-Noble Transition Metal Catalysts: A Review. *Fuel Process. Technol.* **2020**, *199*, 106238.
(49) Contreras, J. L.; Salmones, J.; Colín-Luna, J. A.; Nuño, L.; Quintana, B.; Córdova, I.; Zeifert, B.; Tapia, C.; Fuentes, G. A. Catalysts for H2 Production Using the Ethanol Steam Reforming (a Review). *Int. J. Hydrogen Energy* **2014**, *39* (33), 18835−18853.
(50) Sharma, Y. C.; Kumar, A.; Prasad, R.; Upadhyay, S. N. Ethanol Steam Reforming for Hydrogen Production: Latest and Effective Catalyst Modification Strategies to Minimize Carbonaceous Deactivation. *Renewable and Sustainable Energy Reviews* **2017**, *74*, 89−103.
(51) Ni, M.; Leung, D. Y. C.; Leung, M. K. H. A Review on Reforming Bio-Ethanol for Hydrogen Production. *Int. J. Hydrogen Energy* **2007**, *32* (15), 3238−3247.
(52) Taghizadeh, M.; Aghili, F. Recent Advances in Membrane Reactors for Hydrogen Production by Steam Reforming of Ethanol as a Renewable Resource. *Reviews in Chemical Engineering* **2019**, *35* (3), 377−392.
(53) Iulianelli, A.; Basile, A. Hydrogen Production from Ethanol via Inorganic Membrane Reactors Technology: A Review. *Catalysis Science and Technology.* **2011**, *1*, 366−379.
(54) Ma, Y.; Wang, X. R.; Li, T.; Zhang, J.; Gao, J.; Sun, Z. Y. Hydrogen and Ethanol: Production, Storage, and Transportation. *Int. J. Hydrogen Energy* **2021**, *46* (54), 27330−27348.
(55) Ramsey, S.; Williams, B.; Jarrell, P.; Hubbs, T. *Economic Research Service Special Outlook Report Number BIO-05 Global Demand for Fuel Ethanol Through 2030*, 2023. www.ers.usda.gov.
(56) U. S. Department of Energy. *Alternative Fuel Data Center*. https://afdc.energy.gov/.
(57) de Lima, L. M.; Bacchi, M. R. P. Chapter 13 - Global Ethanol Market: Commercialization Trends, Regulations, and Key Drivers. In *Advances in Sugarcane Biorefinery*; Chandel, A. K., Luciano Silveira, M. H., Eds.; Elsevier, 2018; pp 253−277. DOI: 10.1016/B978-0-12-804534-3.00013-6.
(58) Mussatto, S. I.; Dragone, G.; Guimarães, P. M. R.; Silva, J. P. A.; Carneiro, L. M.; Roberto, I. C.; Vicente, A.; Domingues, L.; Teixeira, J. A. Technological Trends, Global Market, and Challenges of Bio-Ethanol Production. *Biotechnol Adv.* **2010**, *28* (6), 817−830.
(59) Sikarwar, V. S.; Zhao, M.; Fennell, P. S.; Shah, N.; Anthony, E. J. Progress in Biofuel Production from Gasification. *Prog. Energy Combust. Sci.* **2017**, *61*, 189−248.
(60) Subramani, V.; Gangwal, S. K. A Review of Recent Literature to Search for an Efficient Catalytic Process for the Conversion of Syngas to Ethanol. *Energy Fuels* **2008**, *22* (2), 814−839.
(61) Kothari, R.; Buddhi, D.; Sawhney, R. L. Comparison of Environmental and Economic Aspects of Various Hydrogen Production Methods. *Renewable and Sustainable Energy Reviews* **2008**, *12*, 553−563.
(62) Nikolaidis, P.; Poullikkas, A. A Comparative Overview of Hydrogen Production Processes. *Renewable and Sustainable Energy Reviews.* **2017**, *67*, 597−611.
(63) Midilli, A.; Kucuk, H.; Topal, M. E.; Akbulut, U.; Dincer, I. A Comprehensive Review on Hydrogen Production from Coal Gasification: Challenges and Opportunities. *International Journal of Hydrogen Energy.* **2021**, *46*, 25385−25412.
(64) Chaubey, R.; Sahu, S.; James, O. O.; Maity, S. A Review on Development of Industrial Processes and Emerging Techniques for Production of Hydrogen from Renewable and Sustainable Sources. *Renewable and Sustainable Energy Reviews* **2013**, *23*, 443−462.
(65) Ma, R.; Xu, B.; Zhang, X. Catalytic Partial Oxidation (CPOX) of Natural Gas and Renewable Hydrocarbons/Oxygenated Hydrocarbons—A Review. *Catal. Today* **2019**, *338*, 18−30.
(66) Du, Z.; Liu, C.; Zhai, J.; Guo, X.; Xiong, Y.; Su, W.; He, G. A Review of Hydrogen Purification Technologies for Fuel Cell Vehicles. *Catalysts* **2021**, *11* (3), 393.
(67) Amin, M.; Butt, A. S.; Ahmad, J.; Lee, C.; Azam, S. U.; Mannan, H. A.; Naveed, A. B.; Farooqi, Z. U. R.; Chung, E.; Iqbal, A. Issues and Challenges in Hydrogen Separation Technologies. *Energy Reports* **2023**, *9*, 894−911.
(68) Bernardo, G.; Araújo, T.; da Silva Lopes, T.; Sousa, J.; Mendes, A. Recent Advances in Membrane Technologies for Hydrogen Purification. *Int. J. Hydrogen Energy* **2020**, *45* (12), 7313−7338.
(69) Basile, A.; Liguori, S.; Iulianelli, A. Membrane Reactors for Methane Steam Reforming (MSR). In *Membrane Reactors for Energy Applications and Basic Chemical Production*; Elsevier Inc., 2015; pp 31−59. DOI: 10.1016/B978-1-78242-223-5.00002-9.
(70) Steinberg, M.; Cheng, H. C. Modern and Prospective Technologies for Hydrogen Production from Fossil Fuels. *Int. J. Hydrogen Energy* **1989**, *14* (11), 797−820.
(71) Wee, S. L.; Tye, C. T.; Bhatia, S. Membrane Separation Process-Pervaporation through Zeolite Membrane. *Separation and Purification Technology.* **2008**, *63*, 500−516.
(72) Kargari, A.; Rezaeinia, S. State-of-the-Art Modification of Polymeric Membranes by PEO and PEG for Carbon Dioxide Separation: A Review of the Current Status and Future Perspectives. *Journal of Industrial and Engineering Chemistry.* **2020**, *84*, 1−22.
(73) Yong, W. F.; Zhang, H. Recent Advances in Polymer Blend Membranes for Gas Separation and Pervaporation. *Progress in Materials Science.* **2021**, *116*, 100713.
(74) Li, P.; Wang, Z.; Qiao, Z.; Liu, Y.; Cao, X.; Li, W.; Wang, J.; Wang, S. Recent Developments in Membranes for Efficient Hydrogen Purification. *J. Membr. Sci.* **2015**, *495*, 130−168.
(75) Sidhikku Kandath Valappil, R.; Ghasem, N.; Al-Marzouqi, M. Current and Future Trends in Polymer Membrane-Based Gas Separation Technology: A Comprehensive Review. *Journal of Industrial and Engineering Chemistry* **2021**, *98*, 103−129.
(76) Khulbe, K. C.; Matsuura, T.; Feng, C. Y.; Ismail, A. F. Recent Development on the Effect of Water/Moisture on the Performance of Zeolite Membrane and MMMs Containing Zeolite for Gas Separation; Review. *RSC Adv.* **2016**, *6*, 42943−42961.
(77) Makertihartha, I. G. B. N.; Zunita, M.; Rizki, Z.; Dharmawijaya, P. T. Advances of Zeolite Based Membrane for Hydrogen Production via Water Gas Shift Reaction. *J. Phys. Conf Ser.* **2017**, *877* (1), No. 012076.
(78) Feng, C.; Khulbe, K. C.; Matsuura, T.; Farnood, R.; Ismail, A. F. Recent Progress in Zeolite/Zeotype Membranes. *Journal of Membrane Science and Research* **2015**, *1* (2), 49−72.
(79) Wang, H.; Wang, X.; Meng, B.; Tan, X.; Loh, K. S.; Sunarso, J.; Liu, S. Perovskite-Based Mixed Protonic−Electronic Conducting Membranes for Hydrogen Separation: Recent Status and Advances. *Journal of Industrial and Engineering Chemistry* **2018**, *60*, 297−306.

(80) Meng, X.; Song, J.; Yang, N.; Meng, B.; Tan, X.; Ma, Z. F.; Li, K. Ni−BaCe0.95Tb0.05O3−δ Cermet Membranes for Hydrogen Permeation. *J. Membr. Sci.* **2012**, *401*−*402*, 300−305.
(81) Balachandran, U.; Lee, T. H.; Chen, L.; Song, S. J.; Picciolo, J. J.; Dorris, S. E. Hydrogen Separation by Dense Cermet Membranes. *Fuel* **2006**, *85* (2), 150−155.
(82) Hu, Z.; Wang, Z.; Wang, M.; Wang, Z.; Chu, Y.; Tan, X.; Hu, Y.; Chen, T.; Liu, S. Low-Cost Iron (Fe) Hollow Fiber Membrane for Hydrogen Separation. *J. Membr. Sci.* **2024**, *706*, No. 122966.
(83) Cooney, D. A.; Way, J. D.; Wolden, C. A. A Comparison of the Performance and Stability of Pd/BCC Metal Composite Membranes for Hydrogen Purification. *Int. J. Hydrogen Energy* **2014**, *39* (33), 19009−19017.
(84) Behr, F.; Kugler, B.; Pietsch, M.; Weirich, W. Non-Porous Hydrogen Diffusion Membrane and Utilization Thereof. US Patent 4,781,734, November 1988.
(85) Wang, M.; Wang, Z.; Tan, X.; Liu, S. Externally Self-Supported Metallic Nickel Hollow Fiber Membranes for Hydrogen Separation. *J. Membr. Sci.* **2022**, *653*, No. 120513.
(86) Xue, K.; Hu, Z.; Li, C.; Wang, M.; Tan, X.; Wang, Z.; Kawi, S.; Meng, X.; Qiu, J.; Liu, S. Hydrogen Production by Glucose Reforming Using a Nickel Hollow Fiber Membrane Reactor. *J. Membr. Sci.* **2024**, *695*, No. 122488.
(87) Deng, C.; Hu, Z.; Wang, M.; Wang, Y.; Wang, Z.; Chen, T.; Tan, X.; Liu, S. Sintering of the Metallic Nickel Hollow Fibers into High-Performance Membranes for H2 Permeation. *Ind. Eng. Chem. Res.* **2023**, *62* (2), 1132−1140.
(88) Eremeev, N.; Krasnov, A.; Bespalko, Y.; Bobrova, L.; Smorygo, O.; Sadykov, V. An Experimental Performance Study of a Catalytic Membrane Reactor for Ethanol Steam Reforming over a Metal Honeycomb Catalyst. *Membranes (Basel)* **2021**, *11* (10), 790.
(89) Dube, S.; Gorimbo, J.; Moyo, M.; Okoye-Chine, C. G.; Liu, X. Synthesis and Application of Ni-Based Membranes in Hydrogen Separation and Purification Systems: A Review. *J. Environ. Chem. Eng.* **2023**, *11* (1), No. 109194.
(90) Pal, N.; Agarwal, M.; Maheshwari, K.; Solanki, Y. S. A Review on Types, Fabrication and Support Material of Hydrogen Separation Membrane. *Mater. Today Proc.* **2020**, *28*, 1386−1391.
(91) Al-Mufachi, N. A.; Rees, N. V.; Steinberger-Wilkens, R. Hydrogen Selective Membranes: A Review of Palladium-Based Dense Metal Membranes. *Renewable and Sustainable Energy Reviews* **2015**, *47*, 540−551.
(92) Rahimpour, M. R.; Samimi, F.; Babapoor, A.; Tohidian, T.; Mohebi, S. Palladium Membranes Applications in Reaction Systems for Hydrogen Separation and Purification: A Review. *Chemical Engineering and Processing: Process Intensification* **2017**, *121*, 24−49.
(93) Deveau, N. D.; Ma, Y. H.; Datta, R. Beyond Sieverts' Law: A Comprehensive Microkinetic Model of Hydrogen Permeation in Dense Metal Membranes. *J. Membr. Sci.* **2013**, *437*, 298−311.
(94) Caravella, A.; Scura, F.; Barbieri, G.; Drioli, E. Sieverts Law Empirical Exponent for Pd-Based Membranes: Critical Analysis in Pure H2 Permeation. *J. Phys. Chem. B* **2010**, *114* (18), 6033−6047.
(95) Anzelmo, B.; Liguori, S.; Mardilovich, I.; Iulianelli, A.; Ma, Y. H.; Wilcox, J.; Basile, A. Fabrication & Performance Study of a Palladium on Alumina Supported Membrane Reactor: Natural Gas Steam Reforming, a Case Study. *Int. J. Hydrogen Energy* **2018**, *43* (15), 7713−7721.
(96) Ma, C.; Wang, M.; Wang, Z.; Gao, M.; Wang, J. Recent Progress on Thin Film Composite Membranes for CO2 Separation. *Journal of CO2 Utilization* **2020**, *42*, No. 101296.
(97) Konsolakis, M.; Ioakimidis, Z.; Kraia, T.; Marnellos, G. E. Hydrogen Production by Ethanol Steam Reforming (ESR) over CeO2 Supported Transition Metal (Fe, Co, Ni, Cu) Catalysts: Insight into the Structure-Activity Relationship. *Catalysts* **2016**, *6* (3), 39.
(98) Shi, K.; An, X.; Wu, X.; Xie, X. Modification Strategies for Enhancing Anti-Coking of Ni-, Co-Based Catalysts during Ethanol Steam Reforming: A Review. *Int. J. Hydrogen Energy* **2022**, *47* (93), 39404−39428.
(99) Gallucci, F.; Basile, A.; Tosti, S.; Iulianelli, A.; Drioli, E. Methanol and Ethanol Steam Reforming in Membrane Reactors: An Experimental Study. *Int. J. Hydrogen Energy* **2007**, *32* (9), 1201−1210.
(100) Sahoo, D. R.; Vajpai, S.; Patel, S.; Pant, K. K. Kinetic Modeling of Steam Reforming of Ethanol for the Production of Hydrogen over Co/Al2O3 Catalyst. *Chem. Eng. J.* **2007**, *125* (3), 139−147.
(101) Akande, A.; Aboudheir, A.; Idem, R.; Dalai, A. Kinetic Modeling of Hydrogen Production by the Catalytic Reforming of Crude Ethanol over a Co-Precipitated Ni-Al2O3 Catalyst in a Packed Bed Tubular Reactor. *Int. J. Hydrogen Energy* **2006**, *31* (12), 1707−1715.
(102) Graschinsky, C.; Laborde, M.; Amadeo, N.; Le Valant, A.; Bion, N.; Epron, F.; Duprez, D. Ethanol Steam Reforming over Rh(1%)MgAl2O4/Al2O3: A Kinetic Study. *Ind. Eng. Chem. Res.* **2010**, *49* (24), 12383−12389.
(103) Rossetti, I.; Compagnoni, M.; Torli, M. Process Simulation and Optimisation of H2 Production from Ethanol Steam Reforming and Its Use in Fuel Cells. 1. Thermodynamic and Kinetic Analysis. *Chem. Eng. J.* **2015**, *281*, 1024−1035.
(104) Lu, P.-J.; Chen, T.-S.; Chern, J.-M. Reaction Network and Kinetic Analysis of Ethanol Steam Reforming over a Ru/Al2O3 Catalyst. *Catal. Today* **2011**, *174* (1), 17−24.
(105) Punase, K. D.; Rao, N.; Vijay, P. A Review on Mechanistic Kinetic Models of Ethanol Steam Reforming for Hydrogen Production Using a Fixed Bed Reactor. *Chemical Papers* **2019**, *73* (5), 1027−1042.
(106) Hedayati, A.; Le Corre, O.; Lacarrière, B.; Llorca, J. Experimental and Exergy Evaluation of Ethanol Catalytic Steam Reforming in a Membrane Reactor. *In Catalysis Today; Elsevier* **2016**, *268*, 68−78.
(107) Miyamoto, M.; Yoshikawa, Y.; Oumi, Y.; Yamaura, S.-i.; Uemiya, S. Effects of Catalysts and Membranes on the Performance of Membrane Reactors in Steam Reforming of Ethanol at Moderate Temperature. *Processes* **2016**, *4* (2), 18.
(108) Iulianelli, A.; Liguori, S.; Vita, A.; Italiano, C.; Fabiano, C.; Huang, Y.; Basile, A. The Oncoming Energy Vector: Hydrogen Produced in Pd-Composite Membrane Reactor via Bioethanol Reforming over Ni/CeO2 Catalyst. *Catal. Today* **2016**, *259* (Part 2), 368−375.
(109) Iulianelli, A.; Palma, V.; Bagnato, G.; Ruocco, C.; Huang, Y.; Veziroğlu, N. T.; Basile, A. From Bioethanol Exploitation to High Grade Hydrogen Generation: Steam Reforming Promoted by a Co-Pt Catalyst in a Pd-Based Membrane Reactor. *Renew Energy* **2018**, *119*, 834−843.
(110) Ma, R.; Castro-Dominguez, B.; Mardilovich, I. P.; Dixon, A. G.; Ma, Y. H. Experimental and Simulation Studies of the Production of Renewable Hydrogen through Ethanol Steam Reforming in a Large-Scale Catalytic Membrane Reactor. *Chem. Eng. J.* **2016**, *303*, 302−313.
(111) Ruocco, C.; Palma, V.; Ricca, A. Hydrogen Production by Oxidative Reforming of Ethanol in a Fluidized Bed Reactor Using a PtNi/CeO2SiO2 Catalyst. *Int. J. Hydrogen Energy* **2019**, *44* (25), 12661−12670.
(112) Santucci, A.; Borgogni, F.; Cordiner, S.; Traversa, E.; Tosti, S. Low Temperature Ethanol Steam Reforming in a Pd-Ag Membrane Reformer. *ECS Trans* **2008**, *6* (17), 29−35.
(113) Mironova, E. Y.; Ermilova, M. M.; Orekhova, N. V.; Basov, N. L.; Yaroslavtsev, A. B. Hydrogen Production by Ethanol Steam Reforming in the Presence of Pd-, Pt-, Ru-, and Ni-Containing Nanodiamonds in Conventional and Membrane Reactors. *Membranes and Membrane Technologies* **2019**, *1* (4), 246−253.
(114) Jia, H.; Zhang, J.; Yu, J.; Yang, X.; Sheng, X.; Xu, H.; Sun, C.; Shen, W.; Goldbach, A. Efficient H2 Production via Membrane-Assisted Ethanol Steam Reforming over Ir/CeO2 Catalyst. *Int. J. Hydrogen Energy* **2019**, *44* (45), 24733−24745.
(115) Jia, H.; Xu, H.; Sheng, X.; Yang, X.; Shen, W.; Goldbach, A. High-Temperature Ethanol Steam Reforming in PdCu Membrane Reactor. *J. Membr. Sci.* **2020**, *605*, 118083.

https://doi.org/10.1021/acs.energyfuels.4c02755
Energy Fuels 2024, 38, 19992−20014

(116) Basile, A.; Gallucci, F.; Iulianelli, A.; De Falco, M.; Liguori, S. Hydrogen Production by Ethanol Steam Reforming: Experimental Study of a Pd-Ag Membrane Reactor and Traditional Reactor Behaviour. *International Journal of Chemical Reactor Engineering* **2008**, DOI: 10.2202/1542-6580.1591.
(117) Basile, A.; Gallucci, F.; Iulianelli, A.; Tosti, S. CO-Free Hydrogen Production by Ethanol Steam Reforming in a Pd-Ag Membrane Reactor. *Fuel Cells* **2008**, *8* (1), 62−68.
(118) Iulianelli, A.; Basile, A. An Experimental Study on Bio-Ethanol Steam Reforming in a Catalytic Membrane Reactor. Part I: Temperature and Sweep-Gas Flow Configuration Effects. *Int. J. Hydrogen Energy* **2010**, *35* (7), 3170−3177.
(119) Iulianelli, A.; Liguori, S.; Longo, T.; Tosti, S.; Pinacci, P.; Basile, A. An Experimental Study on Bio-Ethanol Steam Reforming in a Catalytic Membrane Reactor. Part II: Reaction Pressure, Sweep Factor and WHSV Effects. *Int. J. Hydrogen Energy* **2010**, *35* (7), 3159−3164.
(120) Lim, H.; Gu, Y.; Oyama, S. T. Reaction of Primary and Secondary Products in a Membrane Reactor: Studies of Ethanol Steam Reforming with a Silica-Alumina Composite Membrane. *J. Membr. Sci.* **2010**, *351* (1−2), 149−159.
(121) Lim, H.; Gu, Y.; Oyama, S. T. Studies of the Effect of Pressure and Hydrogen Permeance on the Ethanol Steam Reforming Reaction with Palladium- and Silica-Based Membranes. *J. Membr. Sci.* **2012**, *396*, 119−127.
(122) Seelam, P. K.; Liguori, S.; Iulianelli, A.; Pinacci, P.; Calabrò, V.; Huuhtanen, M.; Keiski, R.; Piemonte, V.; Tosti, S.; De Falco, M.; Basile, A. Hydrogen Production from Bio-Ethanol Steam Reforming Reaction in a Pd/PSS Membrane Reactor. *Catal. Today* **2012**, *193* (1), 42−48.
(123) Basile, A.; Palma, V.; Ruocco, C.; Bagnato, G.; Jokar, S. M.; Rahimpour, M. R.; Shariati, A.; Rossi, C.; Iulianelli, A. Pure Hydrogen Production via Ethanol Steam Reforming Reaction over a Novel Pt-Co Based Catalyst in a Dense Pd-Ag Membrane Reactor (An Experimental Study). *International Journal of Membrane Science and Technology* **2015**, *2* (1), 5−14.
(124) Yu, C. Y.; Lee, D. W.; Park, S. J.; Lee, K. Y.; Lee, K. H. Ethanol Steam Reforming in a Membrane Reactor with Pt-Impregnated Knudsen Membranes. *Appl. Catal., B* **2009**, *86* (3−4), 121−126.
(125) Yun, S.; Lim, H.; Ted Oyama, S. Experimental and Kinetic Studies of the Ethanol Steam Reforming Reaction Equipped with Ultrathin Pd and Pd-Cu Membranes for Improved Conversion and Hydrogen Yield. *J. Membr. Sci.* **2012**, *409−410*, 222−231.
(126) Murmura, M. A.; Patrascu, M.; Annesini, M. C.; Palma, V.; Ruocco, C.; Sheintuch, M. Directing Selectivity of Ethanol Steam Reforming in Membrane Reactors. *Int. J. Hydrogen Energy* **2015**, *40* (17), 5837−5848.
(127) López, E.; Divins, N. J.; Llorca, J. Hydrogen Production from Ethanol over Pd-Rh/CeO 2 with a Metallic Membrane Reactor. *Catal. Today* **2012**, *193*, 145−150.
(128) Domínguez, M.; Taboada, E.; Molins, E.; Llorca, J. Ethanol Steam Reforming at Very Low Temperature over Cobalt Talc in a Membrane Reactor. *Catal. Today* **2012**, *193*, 101−106.
(129) Yu, C. Y.; Lee, D. W.; Park, S. J.; Lee, K. Y.; Lee, K. H. Study on a Catalytic Membrane Reactor for Hydrogen Production from Ethanol Steam Reforming. *Int. J. Hydrogen Energy* **2009**, *34* (7), 2947−2954.
(130) Espinal, R.; Anzola, A.; Adrover, E.; Roig, M.; Chimentao, R.; Medina, F.; López, E.; Borio, D.; Llorca, J. Durable Ethanol Steam Reforming in a Catalytic Membrane Reactor at Moderate Temperature over Cobalt Hydrotalcite. *Int. J. Hydrogen Energy* **2014**, *39* (21), 10902−10910.
(131) Iulianelli, A.; Longo, T.; Liguori, S.; Seelam, P. K.; Keiski, R. L.; Basile, A. Oxidative Steam Reforming of Ethanol over Ru-Al2O3 Catalyst in a Dense Pd-Ag Membrane Reactor to Produce Hydrogen for PEM Fuel Cells. *Int. J. Hydrogen Energy* **2009**, *34* (20), 8558−8565.
(132) Matus, E.; Sukhova, O.; Ismagilov, I.; Kerzhentsev, M.; Stonkus, O.; Ismagilov, Z. Hydrogen Production through Autothermal Reforming of Ethanol: Enhancement of Ni Catalyst Performance via Promotion. *Energies (Basel)* **2021**, *14* (16), 5176.
(133) Wang, W.; Wang, Y. Thermodynamic Analysis of Hydrogen Production via Partial Oxidation of Ethanol. *Int. J. Hydrogen Energy* **2008**, *33* (19), 5035−5044.
(134) Hohn, K. L.; Lin, Y. C. Catalytic Partial Oxidation of Methanol and Ethanol for Hydrogen Generation. *ChemSusChem* **2009**, *2* (10), 927−940.
(135) Li, C.; He, Z.; Ban, X.; Li, N.; Chen, C.; Zhan, Z. Membrane-Based Catalytic Partial Oxidation of Ethanol Coupled with Steam Reforming for Solid Oxide Fuel Cells. *J. Membr. Sci.* **2021**, *622*, No. 119032.
(136) Iulianelli, A.; Liguori, S.; Calabro, V.; Pinacci, P.; Basile, A. Partial Oxidation of Ethanol in a Membrane Reactor for High Purity Hydrogen Production. *Int. J. Hydrogen Energy* **2010**, *35* (22), 12626−12634.
(137) Lin, W. H.; Hsiao, C. S.; Chang, H. F. Effect of Oxygen Addition on the Hydrogen Production from Ethanol Steam Reforming in a Pd-Ag Membrane Reactor. *J. Membr. Sci.* **2008**, *322* (2), 360−367.
(138) Lin, W. H.; Liu, Y. C.; Chang, H. F. Hydrogen Production from Oxidative Steam Reforming of Ethanol in a Palladium-Silver Alloy Composite Membrane Reactor. *Journal of the Chinese Institute of Chemical Engineers* **2008**, *39* (5), 435−440.
(139) Santucci, A.; Annesini, M. C.; Borgognoni, F.; Marrelli, L.; Rega, M.; Tosti, S. Oxidative Steam Reforming of Ethanol over a Pt/Al2O3 Catalyst in a Pd-Based Membrane Reactor. *Int. J. Hydrogen Energy* **2011**, *36* (2), 1503−1511.
(140) Lin, W. H.; Liu, Y. C.; Chang, H. F. Autothermal Reforming of Ethanol in a Pd−Ag/Ni Composite Membrane Reactor. *Int. J. Hydrogen Energy* **2010**, *35* (23), 12961−12969.
(141) Jin, Y.; Rui, Z.; Tian, Y.; Lin, Y. S.; Li, Y. Autothermal Reforming of Ethanol in Dense Oxygen Permeation Membrane Reactor. *Catal. Today* **2016**, *264*, 214−220.
(142) Iulianelli, A.; Ghasemzadeh, K.; Basile, A. Progress in Methanol Steam Reforming Modelling via Membrane Reactors Technology. *Membranes 2018, Vol. 8, Page 65* **2018**, *8* (3), 65.
(143) Habib, M. A.; Haque, M. A.; Harale, A.; Paglieri, S.; Alrashed, F. S.; Al-Sayoud, A.; Nemitallah, M. A.; Hossain, S.; Abuelyamen, A.; Mokheimer, E. M. A.; Ben-Mansour, R. Palladium-Alloy Membrane Reactors for Fuel Reforming and Hydrogen Production: Hydrogen Production Modeling. *Case Studies in Thermal Engineering* **2023**, *49*, No. 103359.
(144) Chen, W.-H.; Li, S.-C.; Lim, S.; Chen, Z.-Y.; Juan, J. C. Reaction and Hydrogen Production Phenomena of Ethanol Steam Reforming in a Catalytic Membrane Reactor. *Energy* **2021**, *220*, No. 119737.
(145) Chen, W.-H.; Chou, W.-S.; Rajendran, S.; Hsu, S.-Y.; Ghorbani, M. Hydrogen Production and Geometry Optimization of Ethanol Steam Reforming Combining Water Gas Shift Reaction in a Crossflow Membrane Tube Reactor. *Int. J. Hydrogen Energy* **2024**, *51*, 637−653.
(146) Saidi, M.; Jahangiri, A. Theoretical Study of Hydrogen Production by Ethanol Steam Reforming: Technical Evaluation and Performance Analysis of Catalytic Membrane Reactor. *Int. J. Hydrogen Energy* **2018**, *43* (32), 15306−15320.
(147) Gallucci, F.; De Falco, M.; Tosti, S.; Marrelli, L.; Basile, A. Ethanol Steam Reforming in a Dense Pd−Ag Membrane Reactor: A Modelling Work. Comparison with the Traditional System. *Int. J. Hydrogen Energy* **2008**, *33* (2), 644−651.
(148) Papadias, D. D.; Lee, S. H. D.; Ferrandon, M.; Ahmed, S. An Analytical and Experimental Investigation of High-Pressure Catalytic Steam Reforming of Ethanol in a Hydrogen Selective Membrane Reactor. *Int. J. Hydrogen Energy* **2010**, *35* (5), 2004−2017.
(149) Koch, R.; López, E.; Divins, N. J.; Allué, M.; Jossen, A.; Riera, J.; Llorca, J. Ethanol Catalytic Membrane Reformer for Direct PEM FC Feeding. *Int. J. Hydrogen Energy* **2013**, *38* (14), 5605−5615.

(150) Zeynali, R.; Khalili, S. S.; Pezeshki, Z.; Akbari, M.; Soleymani, H.; Samimi-Sohrforozani, E.; Safaei, B. Investigating the Effects of Operating Parameters on the Performance of Sorption-Enhanced Membrane Reactor for Ethanol Steam Reforming Reaction Using Computational Fluid Dynamics Method. *Phys. Fluids* **2023**, *35* (10), 107114.
(151) Bobrova, L.; Vernikovskaya, N.; Eremeev, N.; Sadykov, V. Model-Based Performance Analysis of Membrane Reactor with Ethanol Steam Reforming over a Monolith. *Membranes 2022, Vol. 12, Page 741* **2022**, *12* (8), 741.
(152) Bobrova, L.; Eremeev, N.; Vernikovskaya, N.; Sadykov, V.; Smorygo, O. Effect of Asymmetric Membrane Structure on Hydrogen Transport Resistance and Performance of a Catalytic Membrane Reactor for Ethanol Steam Reforming. *Membranes 2021, Vol. 11, Page 332* **2021**, *11* (5), 332.
(153) Ma, R.; Castro-Dominguez, B.; Dixon, A. G.; Ma, Y. H. CFD Study of Heat and Mass Transfer in Ethanol Steam Reforming in a Catalytic Membrane Reactor. *Int. J. Hydrogen Energy* **2018**, *43* (15), 7662−7674.
(154) Hedayati, A.; Le Corre, O.; Lacarrière, B.; Llorca, J. Dynamic Simulation of Pure Hydrogen Production via Ethanol Steam Reforming in a Catalytic Membrane Reactor. *Energy* **2016**, *117*, 316−324.
(155) Gallucci, F.; Van Sint Annaland, M.; Kuipers, J. A. M. Pure Hydrogen Production via Autothermal Reforming of Ethanol in a Fluidized Bed Membrane Reactor: A Simulation Study. *Int. J. Hydrogen Energy* **2010**, *35* (4), 1659−1668.
(156) Spallina, V.; Matturro, G.; Ruocco, C.; Meloni, E.; Palma, V.; Fernandez, E.; Melendez, J.; Pacheco Tanaka, A. D.; Viviente Sole, J. L.; van Sint Annaland, M.; Gallucci, F. Direct Route from Ethanol to Pure Hydrogen through Autothermal Reforming in a Membrane Reactor: Experimental Demonstration, Reactor Modelling and Design. *Energy* **2018**, *143*, 666−681.
(157) Bespalko, Y.; Sadykov, V.; Eremeev, N.; Skryabin, P.; Krieger, T.; Sadovskaya, E.; Bobrova, L.; Uvarov, N.; Lukashevich, A.; Krasnov, A.; Fedorova, Y. Synthesis of Tungstates/Ni0.5Cu0.5O Nanocomposite Materials for Hydrogen Separation Cermet Membranes. *Compos Struct* **2018**, *202*, 1263−1274.
(158) Sadykov, V. A.; Bespalko, Y. N.; Krasnov, A. V.; Skriabin, P. I.; Lukashevich, A. I.; Fedorova, Y. E.; Sadovskaya, E. M.; Eremeev, N. F.; Krieger, T. A.; Ishchenko, A. V.; Belyaev, V. D.; Uvarov, N. F.; Ulihin, A. S.; Skovorodin, I. N. Novel Proton-Conducting Nanocomposites for Hydrogen Separation Membranes. *Solid State Ion* **2018**, *322*, 69−78.
(159) Mas, V.; Bergamini, M. L.; Baronetti, G.; Amadeo, N.; Laborde, M. A Kinetic Study of Ethanol Steam Reforming Using a Nickel Based Catalyst. *Top Catal* **2008**, *51* (1−4), 39−48.
(160) Israni, S. H.; Harold, M. P. Methanol Steam Reforming in Single-Fiber Packed Bed Pd−Ag Membrane Reactor: Experiments and Modeling. *J. Membr. Sci.* **2011**, *369* (1−2), 375−387.
(161) Bakhtyari, A.; Bardool, R.; Rahimpour, M. R.; Mofarahi, M.; Lee, C. H. Performance Analysis and Artificial Intelligence Modeling for Enhanced Hydrogen Production by Catalytic Bio-Alcohol Reforming in a Membrane-Assisted Reactor. *Chem. Eng. Sci.* **2023**, *268*, No. 118432.
(162) Wang, B.; Yu, X.; Chang, J.; Huang, R.; Li, Z.; Wang, H. Techno-Economic Analysis and Optimization of a Novel Hybrid Solar-Wind-Bioethanol Hydrogen Production System via Membrane Reactor. *Energy Convers Manag* **2022**, *252*, No. 115088.
(163) Khamhaeng, P.; Laosiripojana, N.; Assabumrungrat, S.; Kim-Lohsoontorn, P. Techno-Economic Analysis of Hydrogen Production from Dehydrogenation and Steam Reforming of Ethanol for Carbon Dioxide Conversion to Methanol. *Int. J. Hydrogen Energy* **2021**, *46* (60), 30891−30902.
(164) Yukesh Kannah, R.; Kavitha, S.; Preethi; Parthiba Karthikeyan, O.; Kumar, G.; Dai-Viet, N. V.; Rajesh Banu, J. Techno-Economic Assessment of Various Hydrogen Production Methods − A Review. *Bioresour. Technol.* **2021**, *319*, 124175.
(165) Susmozas, A.; Iribarren, D.; Dufour, J. Assessing the Life-Cycle Performance of Hydrogen Production via Biofuel Reforming in Europe. *Resources* **2015**, *4* (2), 398−411.
(166) Khila, Z.; Baccar, I.; Jemel, I.; Hajjaji, N. Thermo-Environmental Life Cycle Assessment of Hydrogen Production by Autothermal Reforming of Bioethanol. *Energy for Sustainable Development* **2017**, *37*, 66−78.
(167) Siddiqui, O.; Dincer, I. A Well to Pump Life Cycle Environmental Impact Assessment of Some Hydrogen Production Routes. *Int. J. Hydrogen Energy* **2019**, *44* (12), 5773−5786.
(168) Cetinkaya, E.; Dincer, I.; Naterer, G. F. Life Cycle Assessment of Various Hydrogen Production Methods. *Int. J. Hydrogen Energy* **2012**, *37* (3), 2071−2080.
(169) Jazani, O.; Elharati, M. A.; Liguori, S. Effects of Porous Supports and Binary Gases on Hydrogen Permeation in Pd−Ag−Y Alloy Membrane. *J. Membr. Sci.* **2025**, *713*, No. 123327.
(170) Bosko, M. L.; Dalla Fontana, A.; Tarditi, A.; Cornaglia, L. Advances in Hydrogen Selective Membranes Based on Palladium Ternary Alloys. *Int. J. Hydrogen Energy* **2021**, *46* (29), 15572−15594.
(171) Peters, T. A.; Kaleta, T.; Stange, M.; Bredesen, R. Development of Ternary Pd-Ag-TM Alloy Membranes with Improved Sulphur Tolerance. *J. Membr. Sci.* **2013**, *429*, 448−458.
(172) Yun, S.; Ted Oyama, S. Correlations in Palladium Membranes for Hydrogen Separation: A Review. *J. Membr. Sci.* **2011**, *375* (1), 28−45.
(173) Teplyakov, V. Polymeric Membranes for Hydrogen Separation/Purification. *Current Trends and Future Developments on (Bio-) Membranes: New Perspectives on Hydrogen Production, Separation, and Utilization* **2020**, 281−304.
(174) Ramirez-Kantun, M. d. l. A.; Weigelt, F.; Neumann, S.; Shishatskiy, S.; Brinkmann, T. Temperature Stable, Polymeric Thin-Film Composite Membrane for Hydrogen Separation. *J. Membr. Sci.* **2024**, *695*, No. 122519.
(175) Wang, M.; Zhou, Y.; Tan, X.; Gao, J.; Liu, S. Nickel Hollow Fiber Membranes for Hydrogen Separation from Reformate Gases and Water Gas Shift Reactions Operated at High Temperatures. *J. Membr. Sci.* **2019**, *575*, 89−97.
(176) Sanchez, N.; Ruiz, R.; Hacker, V.; Cobo, M. Impact of Bioethanol Impurities on Steam Reforming for Hydrogen Production: A Review. *Int. J. Hydrogen Energy* **2020**, *45* (21), 11923−11942.
(177) Dehdashtijahromi, M.; Binazadeh, M.; Farsi, M. Dynamic Modeling, Optimization and Exergy Analysis of Novel Membrane Reactor for Enhanced Olefin and Pure Hydrogen Production via Heavy Paraffin Dehydrogenation. *Int. J. Hydrogen Energy* **2024**, *51*, 225−242.

https://doi.org/10.1021/acs.energyfuels.4c02755
Energy Fuels 2024, 38, 19992−20014